GLOBAL BIOGEOCHEMICAL CYCLES, VOL. 13, NO 4, PAGES 903-922, DECEMBER 1999

Dynamics of isotopic exchange of carbon dioxide in a Tennessee deciduous forest

David R. Bowling[1]

Department of Environmental, Population, and Organismic Biology, University of Colorado, Boulder

Dennis D. Baldocchi[2]

Atmospheric Turbulence and Diffusion Division, National Oceanic and Atmospheric Administration, Oak Ridge, Tennessee

Russell K. Monson

Department of Environmental, Population, and Organismic Biology, University of Colorado, Boulder

Abstract. The combination of isotopic measurements and micrometeorological flux measurements is a powerful new approach that will likely lead to new insight into the dynamics of CO_2 exchange between terrestrial ecosystems and the atmosphere. Since the biological processes of photosynthesis and respiration modify the stable isotopic signature of atmospheric CO_2 in different ways, measurements of the net fluxes of CO_2, $^{13}CO_2$, and $C^{18}OO$ can be used to investigate the relative contribution of each process to net ecosystem CO_2 exchange. We used two independent approaches to measure isotopic fluxes of CO_2 over a Tennessee oak-maple-hickory forest in summer 1998. These approaches involved (1) a combination of standard eddy covariance with intensive flask sampling, and (2) a modification to the relaxed eddy accumulation technique. Strong isotopic signals associated with photosynthesis and respiration were observed and persisted in forest air despite the potential for mixing due to atmospheric turbulence. Calm nights allowed a buildup of respiratory CO_2 below the canopy and were associated with isotopically depleted forest air in the morning. Windy nights were followed by a relatively more enriched early-morning isotopic signal. Entrainment of air from above the decaying nocturnal boundary layer during daytime mixed layer growth exerted strong control on isotopic composition of forest air, resulting in similar isotope ratios in the late afternoon despite different isotopic starting points following calm or windy nights. The influences of the convective boundary layer and turbulent mixing within the forest cannot be ignored when using isotopes of CO_2 to investigate biological processes.

1. Introduction

Through a number of national and international programs considerable effort and research funding is currently being devoted to the measurement of net ecosystem carbon exchange. These programs rely on eddy covariance (EC) measurements to continuously monitor net ecosystem exchange of CO_2 (NEE) at large spatial scales [e.g., *Goulden et al.*, 1996]. While this approach is of fundamental importance, it does not allow the independent measurement of the component processes of NEE, net photosynthesis (A) and respiration (R, where NEE = A + R).

Stable isotopes in atmospheric CO_2 contain useful information about photosynthesis and respiration since each process affects isotopic composition in different ways. Photosynthesis by all plants discriminates against the heavier ^{13}C isotope, leaving the atmosphere enriched in ^{13}C (with $\delta^{13}C$ near -8‰) relative to plant biomass (near -28‰ for C_3 plants). (By convention, isotope ratios are reported relative to an international standard, where $\delta^{13}C$ (or $\delta^{18}O$) = heavy to light isotope, $^{13}C/^{12}C$ or $^{18}O/^{16}O$. δ is expressed in parts per thousand, ‰.) Since there is apparently no fractionation associated with autotrophic [*Lin and Ehleringer*, 1997; see also *Duranceau et al.*, 1999] or heterotrophic [*Hesterberg and Siegenthaler*, 1991] respiration, respiratory CO_2 produced from metabolism and decomposition of plant biomass is depleted ($\delta^{13}C$ more negative) in $^{13}CO_2$ relative to the atmosphere ($\delta^{13}C$ for respired CO_2 is typically near -26 to -28‰). (CO_2 in this paper refers to bulk CO_2 in the atmosphere (all isotopic forms); $^{13}CO_2$ refers to $^{13}C^{16}O^{16}O$, and

[1]Now at Department of Biology, University of Utah, Salt Lake City.

[2]Now at Department of Environmental Science, Policy and Management, University of California, Berkeley.

Paper number 1999GB900072
0886-6236/99/1999GB900072$12.00

$C^{18}OO$ refers to $^{12}C^{18}O^{16}O$.) Nocturnal respiration by all components of an ecosystem (foliage, stems, roots, and soil heterotrophs) tends to dilute the atmosphere with respect to $^{13}CO_2$, while photosynthetic discrimination enriches it during the day. Thus a diurnal cycle is apparent in $\delta^{13}C$ of CO_2 that reflects the individual contributions of photosynthesis and respiration to NEE.

A similar pattern exists for $\delta^{18}O$. A large proportion of CO_2 that diffuses into a photosynthesizing leaf diffuses back out without being fixed by photosynthesis, after equilibrating isotopically with leaf water via the chloroplastic enzyme carbonic anhydrase [*Williams et al.*, 1996]. Transpiration is an evaporative and thus fractionating process, and leaf water shows substantial diurnal enrichment in $\delta^{18}O$ [*Flanagan et al.*, 1991; *Wang and Yakir*, 1995]. Thus CO_2 associated with photosynthesizing leaves is labeled by the oxygen isotopic composition of enriched leaf water. Soil-respired CO_2 approaches isotopic equilibrium with water in the upper layers of the soil profile, since diffusion through the soil pore space is slow relative to the time required for isotopic exchange [*Hesterberg and Siegenthaler*, 1991; *Tans*, 1998; *Miller et al.*, 1999]. Soil water and leaf water usually differ substantially in isotopic composition, and so the CO_2 interacting with each pool reflects this difference. The $\delta^{18}O$ in most systems shows a strong diurnal pattern similar to that of $\delta^{13}C$; respiration tends to dilute atmospheric CO_2 with respect to the heavier isotope $C^{18}OO$, while photosynthesis enriches it.

To use isotopes to directly partition NEE, we require measurements of the isotopic fluxes of $^{13}CO_2$ and $C^{18}OO$. *Yakir and Wang* [1996] have successfully partitioned NEE into A and R for several crop species using the flux-gradient method. However, the gradient approach is difficult to use above or within a tall forest canopy, as the flux-profile relationships on which it is based are only valid above the roughness sublayer at vertical distances 2-3 times canopy height [*Kaimal and Finnigan*, 1994; *Cellier and Brunet*, 1992]. Very few measurement towers over forests extend to these heights, and isotopic gradients for CO_2 in the surface layer over forests are often smaller than required for confident resolution of fluxes [*Lloyd et al.*, 1996].

We introduce in this paper a simple way to use flask sampling combined with eddy covariance to calculate $^{13}CO_2$ flux and, with larger uncertainty, $C^{18}OO$ flux. Additionally, we describe measurements using a recent modification to the relaxed eddy accumulation technique which provide an independent (and significantly more difficult) measurement of $^{13}CO_2$ and $C^{18}OO$ flux. We used these measurements and others to investigate the dynamics of CO_2 exchange in a Tennessee deciduous forest. Relevant theory to partition NEE into its component fluxes will be described and combined with these measurements in a future paper.

2. Materials and Methods

2.1. Site Description

This study was conducted during July 1998 at the Walker Branch Watershed in eastern Tennessee (see *Johnson and van Hook* [1989] or http://www.esd.ornl.gov/programs/WBW/ for further details of the site). Data are presented here for 5 intensive days over a 1-week period from July 11 to July 17. This forest is dominated by oaks (*Quercus alba, Q. prinus*), maples (*Acer rubrum, A. saccharum*), tulip poplar (*Liriodendron tulipifera*), and hickory (*Carya* spp.) [*Hanson et al.*, 1998; *Guenther et al.*, 1996]. Forest canopy height during this study was 26-28 m. Instruments were mounted on a 44-m tower at the western edge of the watershed [*Baldocchi and Harley*, 1995].

2.2. Forest Meteorological Parameters

Net radiation was measured above the canopy using a net radiometer (model 6, Radiation Energy Balance Systems, Seattle, Washington). Relative humidity and air temperature were monitored at three heights using humitters (HMP 35D, Vaisala, Woburn, Massachusetts) equipped with aspirated shields (43408-2, RM Young, Traverse City, Michigan). These heights were chosen at the canopy top (28.5 m), middle (19 m), and approximate bottom of the overstory (10.5 m). The overstory/understory boundary at this site is not well defined, and the 10.5 m height was selected based on the location of the lowest foliage on the trees surrounding the tower. Water vapor density was calculated from the humitter data.

2.3. Eddy Covariance and Canopy Storage Fluxes

Fluxes of sensible and latent heat and CO_2 were measured at 37 m using a triaxial sonic anemometer (SWS-211/3K, Applied Technologies, Inc., Boulder, Colorado) and an open path infrared gas analyzer (IRGA) as described by *Baldocchi and Harley* [1995]. The measurements were aligned with the mean wind streamlines [*Baldocchi et al.*, 1988], and standard density corrections [*Webb et al.*, 1980] were applied. EC fluxes were calculated as $F = \rho\langle w'C'\rangle$, where F represents flux of sensible heat, latent heat, or CO_2, ρ is air density, w is vertical wind velocity, C is CO_2 mixing ratio (or temperature or water vapor), $\langle\rangle$ represents Reynolds averaging, and the primes represent deviation from the Reynolds average [e.g., *Baldocchi et al.*, 1988]. Mean CO_2 mixing ratios were measured at 36, 18, 10, and 0.75 m to compute canopy CO_2 storage as described by *Baldocchi* [1997]. Eddy covariance and storage fluxes are reported as 30-min averages. We use the convention that upward fluxes are positive and the standard definition of net ecosystem exchange, $NEE = \rho\langle w'C'\rangle + dC_i/dt$.

2.4. Flask Sampling

A second CO_2 height-profiler system was used to collect whole-air flask samples at a variety of heights (0.75, 2, 4, 10, 26, and 44 m) for CO_2 mixing and isotope ratio analyses. This system consisted of a closed-path IRGA in absolute mode (6251, Li-Cor, Lincoln, Nebraska), a selection of valves (4-178-900, General Valve, Fairfield, New Jersey), Teflon or polyethylene (3/8" outer diameter, Dekoron 1300, GWS Supply, Appleton, Wisconsin) tubing, and associated electronics and plumbing. Air was constantly pulled through all six inlet lines with a pump (N815KTE, KNF Neuberger, Trenton, New Jersey). A second pump (118.30.00005, KNF) was used to pull a subsample from one of these lines through a 500-mL magnesium perchlorate water trap, through the flask, then through the IRGA. The $Mg(ClO_4)_2$ was changed twice daily

to avoid potential changes in oxygen isotope ratio with saturated desiccant. This system was located in an instrument hut at the base of the tower. Calibrations were performed several times daily using a CO_2-ultra pure-air mixture (Scott-Marrin, Riverside, California) calibrated against a World Meteorological Organization (WMO) primary CO_2 standard, and ultra-pure air (Scott-Marrin, Riverside, California). We used 2.5-L glass flasks from the National Oceanic and Atmospheric Administration / Climate Monitoring and Diagnostics Laboratory global flask network (NOAA-102, Precision Glass Blowing, Englewood, Colorado). Laboratory CO_2 mixing ratio tests suggested that flasks which are under vacuum for extended periods (weeks) can be low by a few μmol mol^{-1} once filled. We therefore filled flasks with dried ambient air in Boulder, Colorado, prior to each experiment. A few hours before use, they were moderately evacuated (< 1 kPa). During sampling, each flask was slowly filled from the selected height over a few minutes, then flushed for at least 5 min.

Flask samples were collected during selected relaxed eddy accumulation (REA) periods on July 14 and 17, at the canopy top (26 m). On July 15, three flasks were filled during each REA period, at 0.75, 26, and 44 m. Samples were also collected at night at a variety of heights on July 13 and 14. CO_2 and N_2O mixing ratio measurements on the flasks were made as described by *Conway et al.* [1994] and *Hofmann et al.* [1998], and all flasks were analyzed for carbon and oxygen isotope ratio in CO_2 after Trolier et al. [1996]. All carbon and oxygen isotope ratios in this paper are reported versus the VPDB-CO_2 standard as described by Trolier et al. [1996]. Precision for the flask measurements is 0.1 μmol mol^{-1} for CO_2, 0.03‰ for $\delta^{13}C$, and 0.05‰ for $\delta^{18}O$. CH_4, CO, and H_2 in flasks were analyzed as described by *Dlugokencky et al.* [1994] and *Novelli et al.* [1992, 1998].

2.5. Eddy Covariance Combined with Flask Sampling

Since early work by *Keeling* [1958], it has been recognized that $\delta^{13}C$ and the reciprocal of C are linearly related (such plots have come to be called Keeling plots). Over the narrow range of observed C within a forest (340-460 μmol mol^{-1} at Walker Branch during this study), $\delta^{13}C$ is also strongly linearly related to C [*Friedli et al.*, 1987; *Flanagan et al.*, 1996], so

$$\delta^{13}C = mC + b \quad (1)$$

Unfortunately this correlation is weaker or sometimes nonexistent for ^{18}O [*Flanagan et al.*, 1997; *Nakazawa et al.*, 1997a; *Sternberg et al.*, 1998], since there can be changes in $\delta^{18}O$ without corresponding changes in C, owing to isotopic equilibration between leaf and soil water, and in some cases moss water and dew.

We exploited the $\delta^{13}C$-versus-C relation to predict the isotope ratio of forest CO_2 at short timescales, using the fast measurements of C obtained for standard eddy covariance. The description that follows is for carbon isotopes, but the oxygen equations follow directly. By conservation of mass for $^{13}CO_2$, the EC relation can be expanded for $^{13}CO_2$ by writing

$$^{13}F = \rho < w'(^{13}CO_2)' > = \rho < w'(\delta^{13}C(C))' >$$

$$= \rho < w'((mC + b)(C))' > \quad (2)$$

where ^{13}F is net flux of $^{13}CO_2$. A similar equation can be developed for $C^{18}OO$ flux. In short, we used a slow measurement (flask sampling) to define the relation between isotopic composition and mixing ratio (via m and b), then combined it with a fast measurement of mixing ratio (from the CO_2 time series at 40 m described below), and computed the isotopic flux directly. A critical assumption here is that the $\delta^{13}C$-versus-C relation is valid at all timescales relevant to EC flux measurement. We address this assumption later in this paper.

We used (2) to calculate net $^{13}CO_2$ (and similarly $C^{18}OO$ flux) and refer to it in this paper as the EC/flask method. As with total CO_2, these net flux measurements (^{13}F and similarly, ^{18}F) must be combined with isotopic "storage" measurements over forested sites to adequately characterize net ecosystem exchange. Following *Lloyd et al.* [1996], we expanded the standard definition of NEE to define net ecosystem exchange for $^{13}CO_2$ as $^{13}NEE = \rho<w'((mC+b)(C))'> + d(\delta^{13}C(Ci))/dt$. To compute the isotopic storage term $d(\delta^{13}C(Ci))/dt$ we used the flask samples to directly measure profiles of $\delta^{13}C$ and C on July 15 or computed $\delta^{13}C$ from the CO_2 mixing ratio profiles and the $\delta^{13}C$-versus-C relationship on other days.

2.6. Relaxed Eddy Accumulation

We used a modification to the standard REA technique [*Bowling et al.*, 1999] called hyperbolic REA (HREA) to collect CO_2 in updrafts and downdrafts for isotope ratio analysis. This technique bases updraft/downdraft sampling decisions on turbulent fluctuations of both wind and CO_2. For convenience, we refer to all hyperbolic REA measurements in this paper simply as REA.

For the REA measurements, a second triaxial sonic anemometer (CSAT3, Campbell Scientific, Logan, Utah) and a second eddy covariance system were located at 40 m. This EC system used a closed-path IRGA (6262, Li-Cor, Lincoln, Nebraska) in absolute mode. A pump (1531-107B-G288X, GAST, Benton Harbor, Michigan) pulled air from within 10 cm of the sonic anemometer path through a filter and Teflon tubing (1/4" OD PTFE, Fisher Scientific, Denver, Colorado), some calibration plumbing, and the IRGA sample cell. The flow rate was 9.0 L min^{-1}, sufficient to maintain turbulent flow in the sample lines. Pressure in the sample cell during sampling was generally 90.6 - 90.8 kPa depending on ambient pressure. CO_2 voltage, H_2O voltage, and sample cell pressure and temperature were recorded at 10 Hz. This system was calibrated once daily as described for the profiler system. More frequent calibrations were not possible since the REA sampling method uses a recursive filter to compute σ_c (described below) which would be disrupted by calibration. The sampling pump on the 40 m EC system was turned off at night to prevent damage by condensation of water in the sample cell.

Wind and IRGA data were collected with a CR23X datalogger (Campbell Scientific, Inc., Logan, Utah). Note that this design involved a plumbing delay between an event at the sonic and the corresponding CO_2 signal at the IRGA; this delay was 0.9 s based on cross-correlation analysis of the time series. There was an additional plumbing delay to the REA inlet; this delay was 8.3 s based on a previous manometric

inlet line volume measurement in the laboratory and the measured REA sampling flow rate. Appropriate time buffering of signals was performed by the CR23X, and valve control signals were sent to the REA system accordingly.

The modified REA method [*Bowling et al.*, 1999] requires knowledge of means, turbulent fluctuations, and standard deviations of w and CO_2 time series during sampling; hence a true Reynolds average is impossible. We used a recursive filter [*McMillen*, 1988] to approximate the Reynolds average $<x>$ during data collection via

$$y_i = e^{-\partial t/\tau} y_{i-1} + (1 - e^{-\partial t/\tau}) x_i \quad (3)$$

where x_i is a datum from the original measured time series x at time i, y_i is the filtered data point at time i, δt is the time interval (0.1 s for 10 Hz measurements), and τ is the filter time constant in seconds. The resulting time series y_i approximates the Reynolds average $<x>$ very closely, and thus

$$x_i' = x_i + y_i \quad (4)$$

represents the fluctuation from this average. The variance of a random variable is the Reynolds average of the square of its fluctuations [*Stull*, 1988]

$$\sigma_x^2 = <(x_i')^2> \quad (5)$$

so we approximated the variance of the w or CO_2 time series as

$$(\sigma_x^2)_i = e^{-\partial t/\tau} (\sigma_x^2)_{i-1} + (1 - e^{-\partial t/\tau})(x_i')^2 \quad (6)$$

We used a filter time constant τ of 400 s which has been shown to be quite effective at this site [*Baldocchi and Harley*, 1995]. Roughly 10 time constants are necessary for filter startup so any interruption in the continuous time series (such as for midday calibrations) would prohibit subsequent REA sampling for more than an hour.

Fast (10 Hz) measurements of w and CO_2 were used to determine when an updraft or downdraft was of sufficient magnitude to exceed an arbitrary threshold, intentionally biasing the sampling to maximize the difference in isotopic composition of updrafts and downdrafts. The sampling strategy utilized the asymmetric HREA technique with an asymmetric hole size (H) of 1.1. See *Bowling et al.* [1999] for full details on the hyperbolic sampling technique.

As shown in Figure 1, the REA design was based on cryogenic CO_2 collection from sample air as the air flowed through the system. A downstream pump (1531-107B-G288X, GAST, Benton Harbor, Michigan) isolated by a 500-mL pressure ballast pulled air through four flow paths, called the updraft trap, updraft bypass, downdraft bypass, and downdraft trap lines (left to right in Figure 1). Arrows in Figure 1 indicate the direction of air flow for an updraft (solid arrows for sample air, dashed arrows for zero air). Sample air was pulled from within 10 cm of the CSAT3 sonic anemometer path (adjacent to the EC system inlet) through a filter and Teflon tubing at 400 mL min^{-1} to a T, then split into two (up and down) short flow paths at 200 mL min^{-1} each. Using solenoid valves (4-209-900, General Valve, Fairfield, New Jersey), these sample streams were routed through the updraft trap line and the downdraft bypass line (during an updraft). The manufacturer's listed response time of these valves was fast enough (10 ms open, 2 ms close) for switching at 10 Hz. CO_2-free ultra pure air (Scott-Marrin, Riverside, California) was routed through the updraft bypass and downdraft sample lines (during an updraft), using identical valves plumbed complementary to the first set. This gas was scrubbed of any residual CO_2, H_2O, and N_2O using a molecular sieve trap (13X, Alltech Chromatography, Deerfield, Illinois). Excess pressure on the tank lines was vented through an open line. Fine-scale needle valves (circles with crosses in Figure 1) were used to match flow rates in the four lines to 200 mL min^{-1}, and verified daily by comparing against a single mass flow meter (FC-260, Tylan General, Torrance, California, not shown in Figure 1). Each trap line consisted of a 300-mL glass and Teflon $Mg(ClO_4)_2$ trap to remove water vapor, a mass flow meter (258C, MKS Instruments, Andover, Massachusetts), and a stainless steel cryotrap (described later in this section) immersed in liquid nitrogen (LN_2, -196° C). The mass flow meters were calibrated in series against a soap bubble flowmeter both in the laboratory and at the field site.

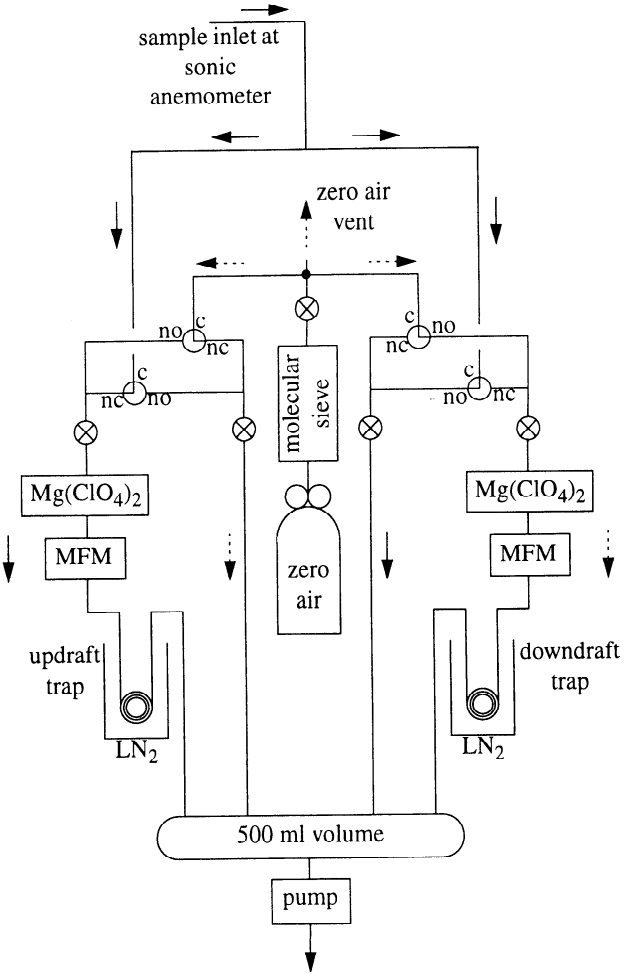

Figure 1. Diagram of the cryogenic REA system used in this study.

Since whole-air samples were not retained, accurate volume measurements were needed to obtain CO_2 mixing ratio. The purpose of the zero air and bypass lines was to provide a constant flow environment for the mass flow meters (MFM)

in the trap lines. These meters are not designed for this purpose. Mass flow meters and controllers generally have response times of the order of seconds, much slower than necessary in this application (<100 ms). Any pressure surges associated with valve switching will not be accurately recorded by the mass flow meters that were used and will produce error in the mixing ratio measurement [*Nie et al.*, 1995; *Valentini et al.*, 1997]. Hence, we plumbed the REA to provide a constant flow environment for the meters, collected flow data at 10 Hz, and parsed the flow data appropriately for updraft and downdraft sampling. In laboratory tests, this system was able to control measured flow to within 0.3% (1σ) of the mean value (range of flows 1.7% of mean). However, it is likely that there were flow surges upon valve switching that were too fast to be recorded by these meters, leading to an overestimation of measured mixing ratio (see description of laboratory tests later in this section).

Considerable attention was paid to the design of the cryotraps. Each trap was made of 5 m of 0.22 cm inner diameter stainless steel tubing (Type 304, Alltech Chromatography, Deerfield, Illinois) coiled as follows. There were seven coil sets, each set consisting of four coils 5 cm in diameter. Four sets were immersed in LN_2, and three were at ambient temperature, alternating cold and warm coil sets. This design was necessary to sample at flow rates fast enough to achieve a measurable sample (1000 mL air sampled) with small time fractions without fractionation. (Time fractions with H=1.1 are near 10% each for updrafts and downdrafts, implying that 80% of sampled air in a given measurement period is rejected [*Bowling et al.*, 1999].) Laboratory tests showed no isotopic fractionation at flow rates as high as 600 ml min $^{-1}$. The tubing assembly was welded to stainless steel bellows toggle valves (SS-4BKT-V52, NUPRO, Willoughby, Ohio) equipped with VCO O-ring fittings, providing a leak-tight trap which could hold a moderate vacuum (10^{-4} kPa) overnight. In early laboratory tests, we had problems with liquid O_2 condensation in the traps. To avoid this, pressure in the CO_2 cryotraps during sampling was reduced to 18 kPa by locating the main pressure drop in the trap line (the needle valve) upstream of the trap.

The collection system was located on the tower at 40 m. Traps were attached to the system, and zero air was flushed through the trap lines for 5-10 min prior to starting a sample. Once the traps were adequately flushed, LN_2 was applied, and the system was left alone on the tower with zero air flushing the traps to avoid human breath interference. A switch at the base of the tower was used to start sampling. All REA samples were collected over a period of 45 min. After sampling, zero air was flushed through the traps until they could be sealed and removed (a few minutes). They were immediately transported to the instrument hut, refrozen in LN_2, and warmed to the temperature of an ethanol dry ice slurry (-78°C), and the condensed CO_2 (and N_2O) were distilled under vacuum (10^{-4} kPa) to a glass tube and sealed with a torch. Noncondensable components were pumped away. Mass of CO_2 in the sample was determined manometrically (0-1.3 kPa barotron, 627A11TAC, MKS Instruments, Andover, Massachusetts) during this transfer in a temperature-controlled glass manifold of known volume. Both up and down transfers were typically finished within 1 hour after sampling. The glass sample tubes were transported back to Boulder and analyzed for carbon and oxygen isotope ratios on a SIRA Series II isotope ratio mass spectrometer (Vacuum Generators, Middlewich, United Kingdom).

The zero air used to flush the traps was scrubbed of N_2O using molecular sieve 13X. In flask samples collected over a broad range of CO_2 mixing ratios (340-440 μmol mol^{-1}), we saw no variation in N_2O (316.0 ± 0.6 nmol mol^{-1}, n=58) at the site. Hence N_2O was not separated from CO_2 during the analyses, and a correction assuming constant N_2O was applied [*Trolier et al.*, 1996]. This correction varies with CO_2 mixing ratio in the sample and is typically less than 0.05‰ for either $\delta^{13}C$ or $\delta^{18}O$.

We used a WMO primary CO_2 standard (365.0 ± 0.1 μmol mol^{-1} CO_2 in air, $\delta^{13}C$ = -8.16 ± 0.01‰, $\delta^{18}O$ = -3.50 ± 0.08‰) in a series of laboratory tests to investigate the accuracy and precision of the cryogenic REA system. Compressed air from this standard tank was pulled through the REA inlet in the same fashion as the zero air in Figure 1. Two types of tests were performed, each with dry tank air and air humidified by bubbling through water. The first type involved sampling tank air continuously through the REA for a fixed time (5-10 min) through the cryotraps, to avoid errors associated with valve switching. The second set involved actual, wind-and-CO_2-directed REA sampling from the CO_2 standard tank, with valves switching as fast as 10 Hz. Good results were obtained for CO_2 mixing ratio with the fixed-time runs (365.0 ± 2.8 μmol mol^{-1} (1σ), n=18). Despite the constant measured flows in the updraft and downdraft trap lines, the accuracy and precision were poor for the REA runs (383.9 ± 11.8 μmol mol^{-1}, n=21). Results for isotope ratios were reasonably good for all the runs ($\delta^{13}C$ = -8.1 ± 0.2‰, $\delta^{18}O$ = -3.5 ± 0.3‰, n=30). However, mass spectrometer precision is almost an order of magnitude better [*Trolier et al.*, 1996]. Hence the isotope measurements with the REA are limited mainly by collection precision and not mass spectrometer precision. There was no relationship between isotope ratio error and mixing ratio error.

Expected differences in updrafts and downdrafts for CO_2 at this site are maximally 6-8 μmol mol^{-1} [*Bowling et al.*, 1999], and so the large error in sample volume measurement prevented measurement of CO_2 mixing ratio directly on the REA isotope ratio samples. We estimated CO_2 mixing ratio in updrafts and downdrafts by parsing the EC time series at 40 m into updrafts and downdrafts, using electronically recorded REA valve control signals and mathematically averaging the resulting "up" and "down" CO_2 time series. Appropriate time shifting was performed to account for the time lag (8.1 s) between the CO_2 signal and REA valve control signals associated with our system design. Density corrections for the presence of water vapor were applied to the raw CO_2 time series [*Pattey et al.*, 1992] (temperature corrections are unnecessary with our EC system design). We conservatively estimate the absolute accuracy of the CO_2 mixing ratio measurements for the REA updrafts and downdrafts as ± 5 μmol mol^{-1}, as there was some voltage drift in the IRGA due to diurnal temperature changes. We stress that while the mean of the time series is known only to ± 5 μmol mol^{-1}, we know how updrafts and downdrafts relate to each other for a given REA sample much better (probably better than ± 0.5

μmol mol^{-1}) because 10 Hz time series for CO_2 are parsed to obtain the mixing ratios in updrafts and downdrafts.

Using the standard REA technique [*Businger and Oncley*, 1990], the flux of CO_2 is calculated as

$$F = \rho < w'C' >= \rho \beta \sigma_w (< C_{up} > - < C_{dn} >) \quad (7)$$

where β is an empirical coefficient (in the range 0.3-0.8), σ_w is the standard deviation of w, and $<C_{up}>$ and $<C_{dn}>$ are the mean CO_2 mixing ratios in the updraft and downdraft reservoirs, respectively. This equation represents mass balance for total CO_2. We can expand this relation for $^{13}CO_2$ by writing

$$^{13}F = \rho \beta \sigma_w (<\delta^{13}C_{up}>< C_{up} > - <\delta^{13}C_{dn}>< C_{dn} >) \quad (8)$$

where $<\delta^{13}C_{up}>$ and $<\delta^{13}C_{dn}>$ are the mean carbon isotopic compositions of updrafts and downdrafts, respectively. A similar equation can be developed for ^{18}F. The β coefficient for total CO_2 flux is calculated from the EC data by rearranging (7) to get

$$\beta = < w'C' > / (\sigma_w (< C_{up} > - < C_{dn} >)) \quad (9)$$

where $<C_{up}>$ and $<C_{dn}>$ are calculated by parsing the fast CO_2 data appropriately and mathematically averaging. We make the assumption that the β coefficient for CO_2 and for $^{13}CO_2$ and $C^{18}OO$ are identical. This is likely a valid assumption since β and σ_w reflect the contribution of atmospheric turbulence to flux, and β is virtually identical for atmospheric trace gases [*Katul et al.*, 1996]. Note that HREA and standard REA differ only in the definition of updrafts and downdrafts (REA thresholds are based on w whereas HREA thresholds are based on w and CO_2).

3. Results and Discussion

3.1. Diurnal Patterns

Trends in CO_2 mixing ratio and isotopic composition for whole-air flask samples collected at the forest floor, canopy top, and above the canopy are shown in Figure 2. There is initially high CO_2 from respiratory buildup at night, followed by a general decrease as the nocturnal boundary layer dissipates and net photosynthesis begins. This is apparent as initially depleted (more negative) isotope ratios that gradually increase through the day. The mixing ratios at canopy top are consistently lower than above the canopy, indicating a strong photosynthetic drawdown of forest CO_2 in the top layers of the canopy. Isotope ratios are most enriched at canopy top, showing the expected effects of photosynthetic discrimination against $^{13}CO_2$ and of interaction between CO_2 and enriched leaf water for $\delta^{18}O$. The respiratory influence is apparent near the forest floor, with high mixing ratios and relatively depleted isotope ratios, especially in the early morning. Oxygen isotopic composition at 44 m (and also at canopy top) varies considerably during the early afternoon; these changes are correlated with changes in wind direction, indicating spatial heterogeneity in the $\delta^{18}O$ signal of forest CO_2. These patterns clearly show the differential influence of photosynthesis and respiration on stable isotopes of forest CO_2 and are consistent with those from other studies [*Flanagan et al.*, 1996, 1997; *Flanagan and Varney* 1995; *Sternberg et al.*, 1997; *Buchmann et al.*, 1997,1998].

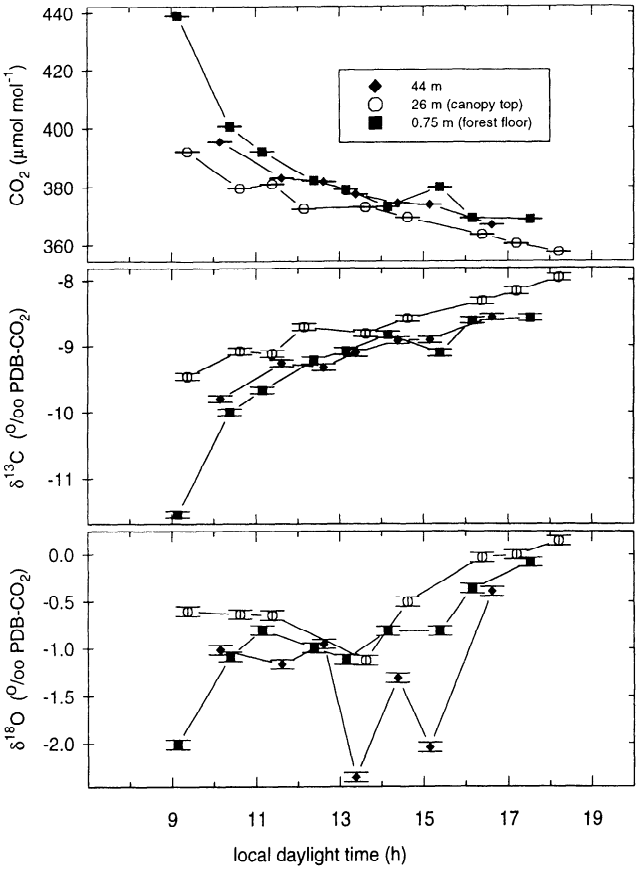

Figure 2. Diurnal trends in whole-air CO_2 mixing ratio, $\delta^{13}C$, and $\delta^{18}O$ from flasks collected at three heights on July 15, 1998.

Figures 3-7 show diurnal patterns in radiation fluxes, net CO_2 exchange, water vapor density gradients within the canopy, and CO_2 mixing and isotope ratios of updrafts and downdrafts from the REA measurements on 5 different days. In Figure 3c, the water vapor gradient within the canopy near the tower was rapidly mixed away about 1000 LT, as a temperature inversion within the upper canopy broke down driven by increasing net radiation. This was accompanied by a burst of latent heat flux above the canopy (Figure 3a) and followed by a negative peak in CO_2 storage flux as the CO_2 gradient was mixed away (Figure 3b). The REA data show a strongly decreasing trend in CO_2 mixing ratio, with downdrafts becoming higher in CO_2 than updrafts (as expected for a photosynthetic flux) as NEE began to increase (more negative) near 1000-1100 LT. Initially, downdrafts were more enriched in $^{13}CO_2$ and $C^{18}OO$ than updrafts, and this pattern reversed about 1200 LT (Figures 3e and 3f). Throughout the afternoon, updrafts remained more enriched in both isotopes than downdrafts; this is expected since updraft air more recently interacted with the photosynthesizing canopy and downdraft air more directly represents the isotopic signature of the well-mixed boundary layer above. This trend should reverse late in the day as the sun sets and net photosynthesis gives way to net respiration.

Note that in Figure 3 the initial $\delta^{13}C$ values were fairly de-

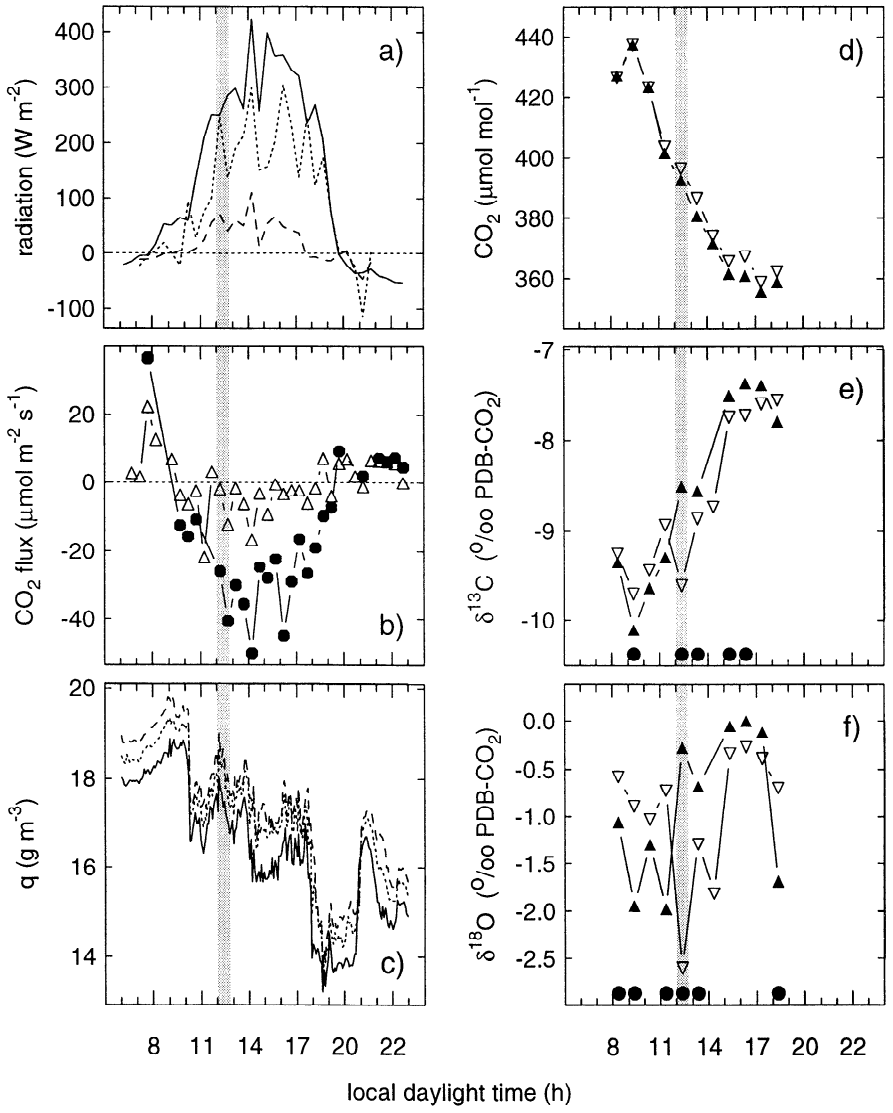

Figure 3. Diurnal trends on July 14, 1998, in (a) net radiation (solid line), latent heat (dotted line), and sensible heat (dashed line) fluxes; (b) NEE (circles) and CO_2 storage (triangles) fluxes; (c) water vapor density at canopy top (28.5 m, solid line), midcanopy (19 m, dotted line), and canopy bottom (10.5 m, dashed line); and (d) CO_2 mixing ratio, (e) $\delta^{13}C$, and (f) $\delta^{18}O$ in REA updrafts (up triangles) and downdrafts (down triangles). Filled circles in Figures 3c and 3f indicate time periods where the difference in updraft and downdraft isotope ratio exceeded measurement uncertainty. Missing REA data are due to human error in sample transfer or analysis; no measurements have been excluded. Shaded vertical bars indicate a strongly convective period as shown in detail for this day's flask samples in Figure 8 and discussed in the text.

pleted and CO_2 mixing ratios were high, indicating a strong respiratory effect on the forest in the early morning. This is contrasted by Figures 4 and 5, which do not show quite as strong a respiratory influence. Friction velocity and potential temperature profiles in the canopy indicated a very stable night preceding July 14 (not shown in Figure 3). Nocturnal conditions for the other days were significantly windier preventing a strong respiratory starting point in the morning. This is followed on these days by a gradual change with the same general pattern but significantly less photosynthetic enrichment ($\delta^{13}C$ changing by 3‰ over the diurnal course in Figure 3 but only by 1‰ on other days).

3.2. Boundary Layer Influences

Integrated NEE and net radiation were very similar on all days. The question arises as to why the forest did not show similar day-to-day magnitudes in isotopic enrichment when it did show similar day-to-day magnitudes in net CO_2 exchange. *Culf et al.* [1997] describe the importance of entrainment in controlling CO_2 mixing ratios over a tropical forest. The nocturnal boundary layer begins to dissipate as the rising sun heats the forest. This dissipation mixes in air from the preceding day's residual mixed layer as the boundary layer grows. The residual layer represents a huge and well-mixed

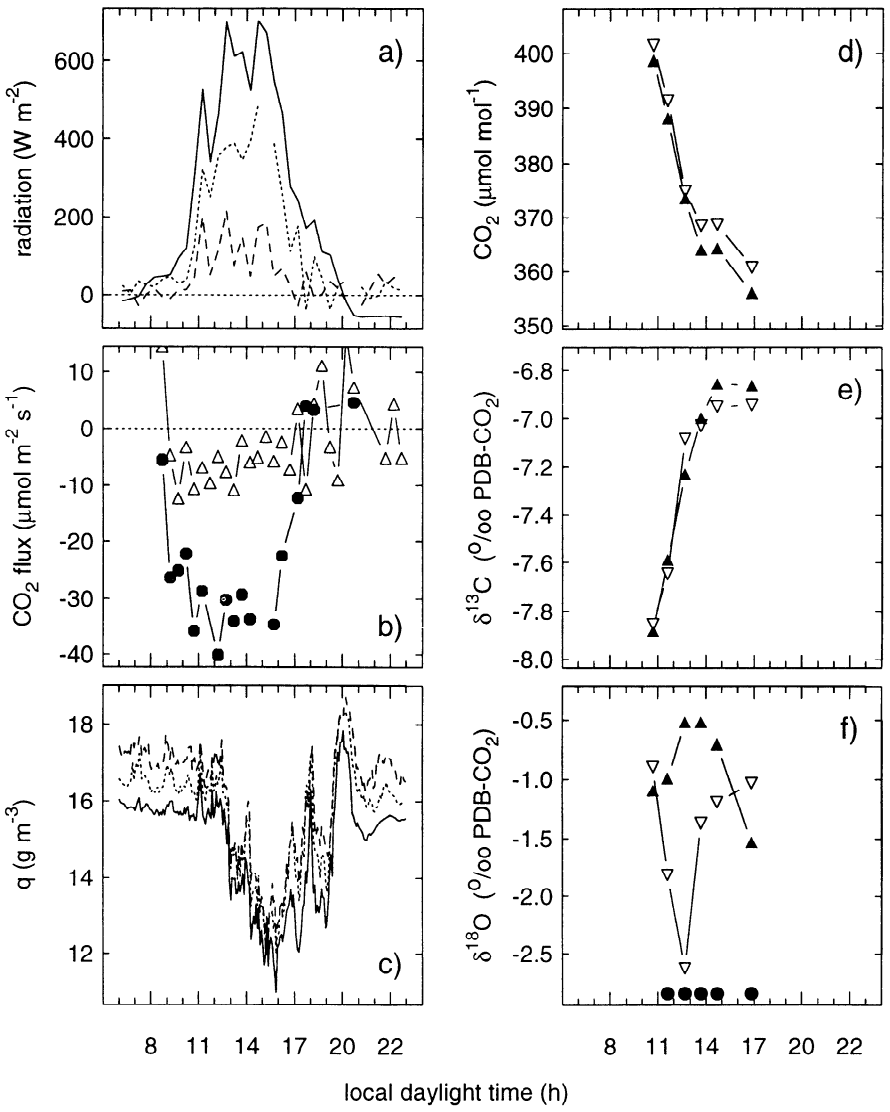

Figure 4. Same as Figure 3, but for July 11, 1998.

volume of air that integrates biospheric effects on the free troposphere over a period of days to weeks. Thus we expect CO_2 mixing ratios in the residual layer to be lower in CO_2 and more enriched in $\delta^{13}C$ (and $\delta^{18}O$ at this site) than the free troposphere [Lloyd et al., 1996; Nakazawa et al., 1997b]. The distinction between the mixed layer and the free troposphere in CO_2 exchange between the biosphere and the atmosphere is an important one that is not always recognized [*Lloyd et al.*, 1996, 1997; *Sternberg et al.*, 1997; *Sternberg et al.*, 1998].

The biospheric influence is mitigated by the large entrainment flux from above. This is also apparent in the humidity data. Note that the water vapor densities in Figures 3 and 7 decrease continually throughout the day despite the fact that the forest produced significant amounts of water through evapotranspiration. Entrainment of drier air from above is likely responsible [*Martin et al.*, 1988; *Davis et al.*, 1997]. Similarly, CO_2 mixing ratios and isotope ratios during strongly convective conditions cannot deviate substantially from those in the well-mixed residual layer which mixes into the convective boundary layer as the day evolves. Thus, in these data, there is a gradual decrease in CO_2 mixing ratio and enrichment in $^{13}CO_2$ that asymptotically approaches the same value each day regardless of starting point [*Culf et al.*, 1997]. Similar patterns in late afternoon CO_2 mixing ratios have been observed from tall towers in North Carolina and Wisconsin [*Bakwin et al.*, 1998a].

An interesting feature of morning boundary layer growth at this site is apparent in Figure 3. Just after 1200 LT, the trend in updraft/downdraft $\delta^{13}C$ and $\delta^{18}O$ reverses abruptly, but this is 2 hours after the onset of net photosynthesis and the breakdown of the local canopy water vapor gradient at the tower. This time period is indicated by shaded vertical bars in Figure 3 and is correlated with a distinct negative peak in the stability parameter $(z\text{-}d)/L$ and several chemical trends as shown in Figure 8. Although CO_2 mixing ratio and $\delta^{13}C$ do not change, there are distinct peaks at the canopy top in meth-

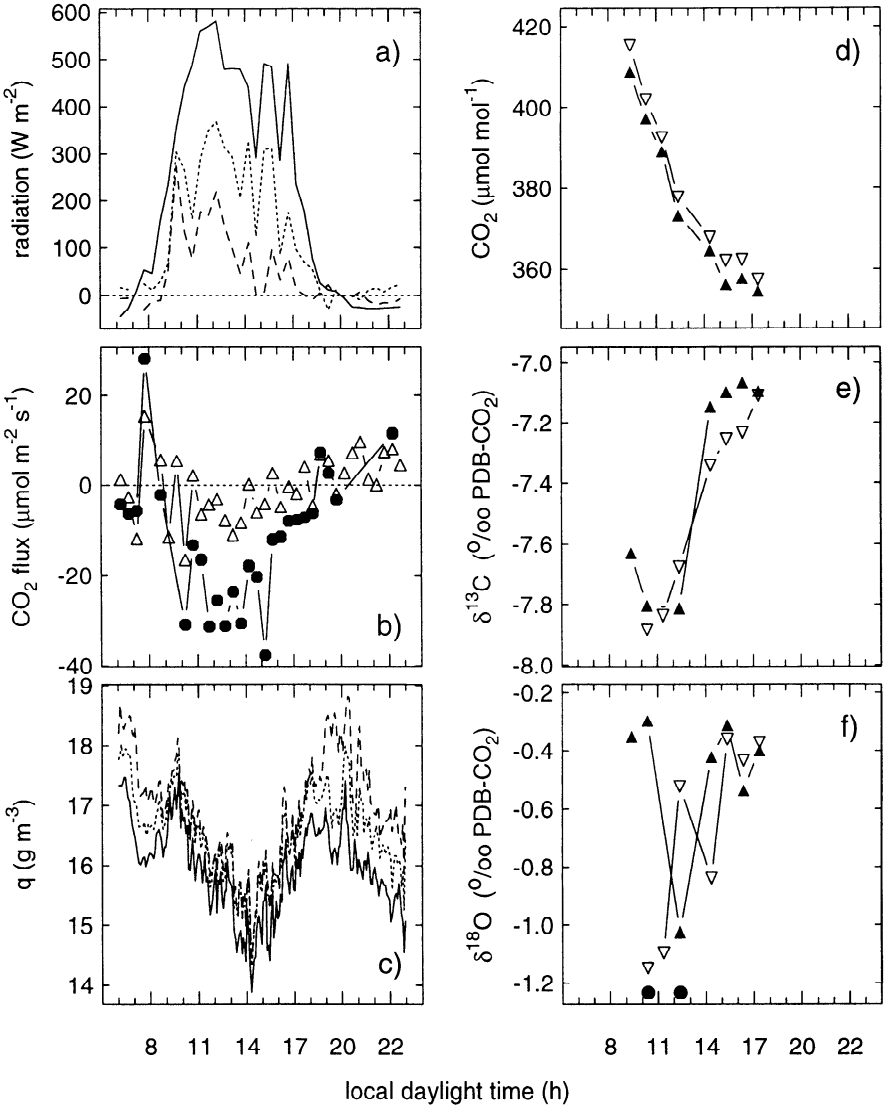

Figure 5. Same as Figure 3, but for July 13, 1998.

ane, nitrous oxide, carbon monoxide, and molecular hydrogen, as well as an abrupt depletion in $\delta^{18}O$. A negative peak in the stability parameter implies light horizontal winds and very strong vertical mixing. This could be associated with rapid boundary layer growth [*Barr and Betts,* 1997], entraining residual layer air in from above as reported for ozone and other pollutants [*Delany et al.*, 1986]. However, $\delta^{18}O$ in the residual layer is likely to be fairly enriched due to the photosynthetic influence near the end of the previous day, but downdraft REA samples and the flasks during this time period were depleted in $C^{18}OO$ (Figures 3 and 8).

A more likely explanation involves the morning boundary layer transition. The tower is located on a ridgetop with roughly 35 m relief over lower lying areas. As the sun rises, the ridgetops should heat up first and exhibit convective activity earlier than the valleys. This is apparent in Figure 3c as the breakdown of canopy stability and mixing of the water vapor gradient at 1000 LT. As the ridgetops continue to heat, strong vertical convection should build and eventually the cooler low-lying valley air should be vigorously mixed into the growing boundary layer, possibly via the ridgetops. This is apparent as a decrease in $\delta^{18}O$ in the flasks at canopy top and in $\delta^{13}C$ and $\delta^{18}O$ of downdrafts (Figures 3e-3f), suggesting that this is a regional phenomenon which affects the entire mixed layer. Low-lying areas near Walker Branch tend to be riparian areas or wetlands, and peaks in CH_4 and N_2O are not surprising. Most of the roads in the area are in the valleys, and thus anthropogenic CO and H_2 would also be expected. This hypothesis is further supported by a concomitant burst of latent heat flux (Figure 3a) that is not associated with changes in net radiation and the observation of transient local canopy air temperature depressions and uphill wind flow below the canopy (data not shown). Negative peaks in $(z\text{-}d)/L$ were observed on 2 other days (shaded bars in Figures 6 and 7) with similar patterns in $\delta^{18}O$ in flasks.

Lenschow et al. [1979] reported a similar event when

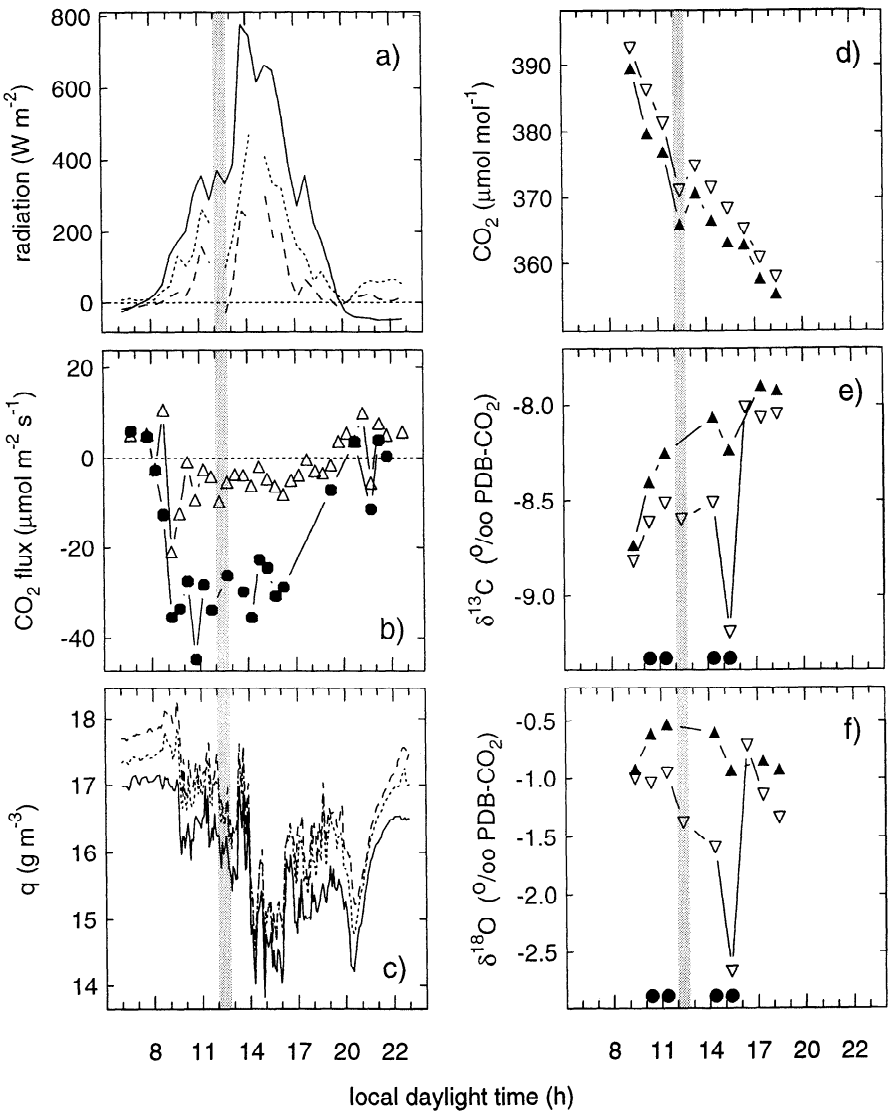

Figure 6. Same as Figure 3, but for July 15, 1998. Flask data from this day are shown in Figure 2.

warm air was mixed into a depression during the morning boundary layer transition and showed that this is a frequent occurrence during the summer in Colorado. *Giez et al.* [1999] used lidar measurements to clearly demonstrate that the development of the boundary layer can be interrupted by advection of cooler air from low-lying areas. Thus the concept of exactly when this deciduous forest becomes "net photosynthetic" seems to be dependent on scale; at the tower this occurs in the morning (near 1000 LT) but over the region it occurs only after all the nocturnal boundary layer air is mixed into the convective boundary layer. If this does occur mainly via preferential vertical flow paths on the ridgetops and it brings a large portion of respiratory CO_2 with it (such as in Figures 7d and 7e), then a possible systematic bias in tower NEE could be apparent at this site.

3.3. Estimating Isotopic Fluxes

The relationship between isotope ratio and mixing ratio is plotted in Figure 9. For $\delta^{13}C$, there is a strong linear relation with CO_2 in the flask samples, with minor differences in daytime versus nighttime. Regression equations for these data are listed in Table 1. Note that the regressions for $\delta^{13}C$ versus CO_2 over this range of CO_2 mixing ratio are just as strong as the traditional *Keeling* [1958] relation ($\delta^{13}C$ versus $1/CO_2$). As expected, the correlations are weaker for $\delta^{18}O$, since there can be variation in $\delta^{18}O$ that is not associated with changes in CO_2 due to isotopic equilibration with liquid water in the surrounding environment [*Sternberg et al.*, 1998].

We wish to combine the information in Figure 9 with eddy covariance data using (2) to calculate isotopic fluxes. A critical assumption of this EC/flask approach is that small measured variations in CO_2 mixing ratio can be used to estimate small variations in $\delta^{13}C$ and $\delta^{18}O$. These parameters are strongly correlated for whole-air flask samples, which integrate the relationships over timescales of minutes to hours. An important question is whether the relationships also hold at shorter timescales relevant to turbulent atmospheric transport of mass (i.e., variations of approximately 100 ms). When

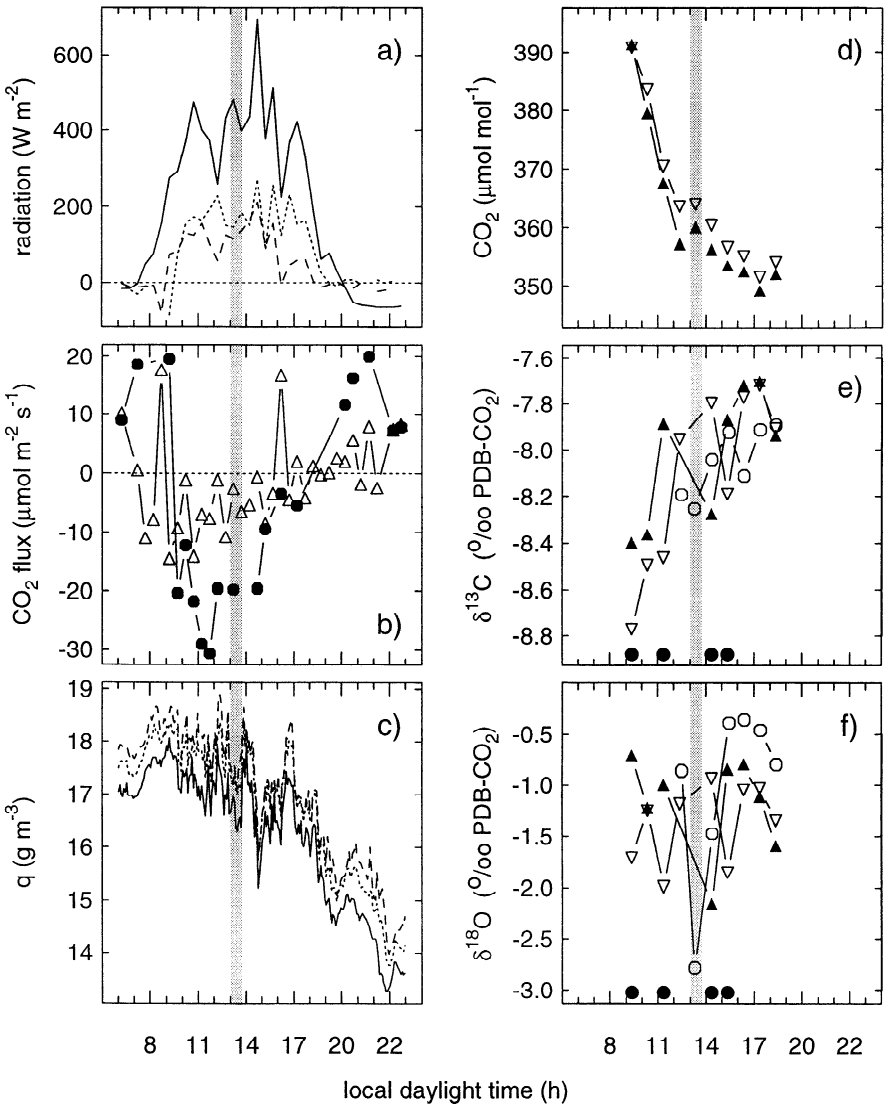

Figure 7. Same as Figure 3, but for July 17, 1998. Flask data collected at canopy top (26 m) for this day have been added to Figures 7d and 7e (circles).

the updraft/downdraft data from the samples collected via REA are plotted (Figure 9), a distinct pattern emerges for $\delta^{13}C$. The relation is still linear, but the slope significantly differs from that of the flask samples. This trend also differs for REA samples on different days (Figure 9; see also regressions for other days in Table 1). The flask samples in Figure 9 were collected over many days, including those shown for the REA data. Sample air in the REA system is routed to the up/down reservoirs as determined by on-line measurement of w and CO_2, and this occurs in "gulps" as short as 100 ms in duration. This linearity may imply that the assumption regarding using CO_2 to estimate $\delta^{13}C$ is valid at short timescales.

At present we do not understand why the slopes are different, but the strong linearity provides confidence that this is not simply an experimental artifact. Tests using standards of known isotopic composition provide a strong indication that the REA system did not fractionate CO_2 during collection. We feel instead that the change in slope is a real phenomenon. There are potentially unknown effects of sampling at short timescales (REA) versus longer timescales (flask sampling), and it could be that changes in source footprint are responsible (flux footprints for this site have been calculated by *Baldocchi et al.*, [1999]). Using the hyperbolic REA sampling protocol [*Bowling et al.*, 1999], the REA samples by nature are biased toward significant updrafts and downdrafts; updrafts represent air more localized in the tower region, while downdrafts represent air from the well- mixed boundary layer above. However, updraft and downdraft samples fall together on the same mixing line (Figure 9). The shorter timescale associated with the REA sample is more representative of the frequencies used in eddy covariance sampling and may be more relevant for use in the EC/flask method. More research is necessary to understand the factors influencing the slopes and to determine the validity of the EC/flask approach.

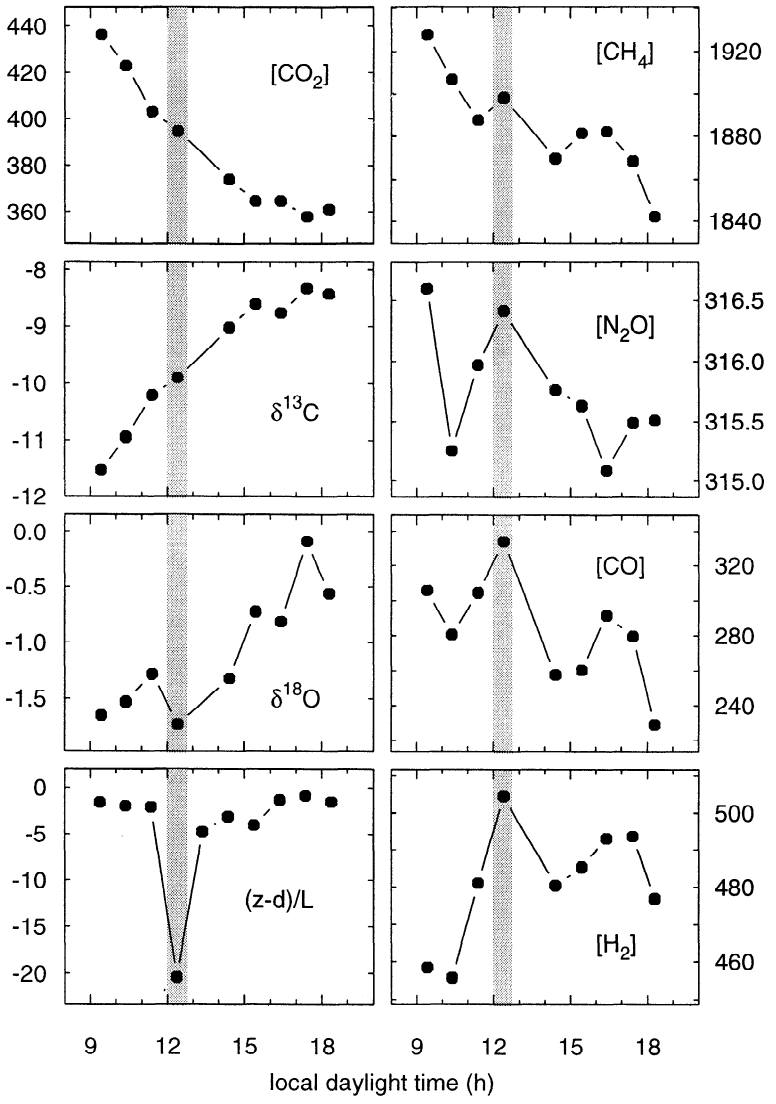

Figure 8. Trends in whole-air flask data at canopy top for July 14, 1998, for $[CO_2]$ (CO_2 mixing ratio, μmol mol^{-1}), $\delta^{13}C$ (‰ PDB-CO_2), $\delta^{18}O$ (‰ PDB-CO_2), the stability parameter $(z\text{-}d)/L$ (dimensionless), $[CH_4]$ (nmol mol^{-1}), $[N_2O]$ (nmol mol^{-1}), [CO] (nmol mol^{-1}), and $[H_2]$ (nmol mol^{-1}). Shaded vertical bars indicate the strong negative peak in $(z\text{-}d)/L$ and correspond to those in Figure 3.

We used the daytime flask regression slope and intercept (Table 1) and (2) to compute the net fluxes of $^{13}CO_2$ shown in Figure 10 (circles). Also shown are net $^{13}CO_2$ fluxes calculated using (2) but with each day's regression from the REA data separately (dashed line) and fluxes measured with the REA approach (squares) using (8). As expected, the use of different slopes provides different results. There is remarkable general agreement between the $^{13}CO_2$ fluxes using the EC/flask and REA methods, both in magnitude and in diurnal pattern. In large part, these methods are based on independent measurements. The isotopic composition measurements for both methods are entirely independent. The CO_2 mixing ratios in updrafts and downdrafts for the REA method were determined from the same CO_2 time series used for the EC/flask method, but this time series was parsed mathematically and averaged to obtain REA updraft and downdraft mixing ratios based on the hyperbolic sampling protocol. A different REA system design with better mixing ratio measurement precision than ours would allow direct mixing ratio measurements on the updraft/downdraft samples and allow these techniques to be fully independent. The EC/flask and REA methods differ substantially in concept and in application and thus the general agreement between them for net $^{13}CO_2$ fluxes provides confidence that they are robust.

The comparison between the two techniques is less appealing for $C^{18}OO$ flux (Figure 11). The EC/flask fluxes are considerably lower than those from the REA method. Since the EC/flask method is based on the relatively poor correlation between $\delta^{18}O$ and CO_2 mixing ratio (Figure 9), the REA technique is likely to be more reliable for measuring net $C^{18}OO$ fluxes. The large uncertainty resulting from the 95% confidence intervals on the flask regression between $\delta^{18}O$ and

Table 1. Keeling and δ-versus-C Geometric Mean Regressions for Flask and REA Samples ($\delta^{13}C$), and for Flask Samples ($\delta^{18}O$).

	m	b	r^2	n
		$\delta^{13}C = m(1/C) + b$		
Flasks				
all flasks	7328	-28.54	0.982	58
night	6341	-26.32	0.952	20
day	6373	-25.93	0.968	38
July 14 day	6262	-25.80	0.994	7
July 15 day	6712	-26.79	0.984	24
July 17 day	4187	-19.78	0.697	7
REA				
all up/down (day)	5211	-21.93	0.480	80
July 11	3649	-16.97	0.950	12
July 13	2497	-14.12	0.947	14
July 14	4837	-21.06	0.885	21
July 15	4385	-20.18	0.466	16
July 17	3199	-16.87	0.705	17
		$\delta^{13}C = m(C) + b$		
Flasks				
all flasks	-0.045	7.934	0.976	58
night	-0.034	3.013	0.963	20
day*	-0.045	8.055	0.969	38
day* (95% confidence)	±0.003	±1.008		
7/14 day	-0.040	6.131	0.993	7
7/15 day	-0.043	7.418	0.979	24
7/17 day	-0.033	3.676	0.701	7
REA				
all up/down (day)	-0.035	5.100	0.490	80
7/11†	-0.025	2.302	0.957	12
7/13†	-0.017	-0.947	0.736	14
7/14†	-0.031	3.592	0.855	21
7/15†	-0.031	3.338	0.361	16
7/17†	-0.023	0.454	0.704	17
		$\delta^{18}O = m(1/C) + b$		
Flasks				
all flasks	4430	-12.69	0.443	58
night	4707	-13.18	0.116	38
day	6483	-18.30	0.005	20
7/14 day	2996	-8.86	0.700	7
7/15 day	5930	-16.50	0.321	24
7/17 day	25162	-71.55	0.512	7
		$\delta^{18}O = m(C) + b$		
Flasks				
all flasks	-0.027	9.358	0.546	58
night	-0.025	8.593	0.194	38
day*	-0.046	16.29	0.112	20
day* (95% confidence)	±0.015	±5.523		
7/14 day	-0.019	6.415	0.666	7
7/15 day	-0.038	13.73	0.306	24
7/17 day	-0.197	69.41	0.516	7

*The daytime flask regressions were used to calculate EC/flask fluxes in Figures 10, 11, and 12.

†The daytime REA regressions were also used to calculate EC/flask fluxes in Figure 10.

CO_2 is shown as error bars on the EC/flask data in Figure 11. However, these error bars do not overlap the REA fluxes, indicating that the regression between $\delta^{18}O$ and CO_2 is perhaps a poor predictor of oxygen isotopic composition of forest CO_2 at short timescales.

Not all collection periods revealed isotopic differences in REA updrafts and downdrafts that exceeded measurement uncertainty (Figures 3-7). Patterns in REA data for both isotopes on all days show a gradual enrichment associated with photosynthesis, with updrafts more enriched than downdrafts as expected. As suggested by earlier simulation results [*Bowling et al.*, 1999], the hyperbolic REA method seems to adequately provide measurable differences in isotope ratio in updrafts and downdrafts in most cases. Resolution of differ-

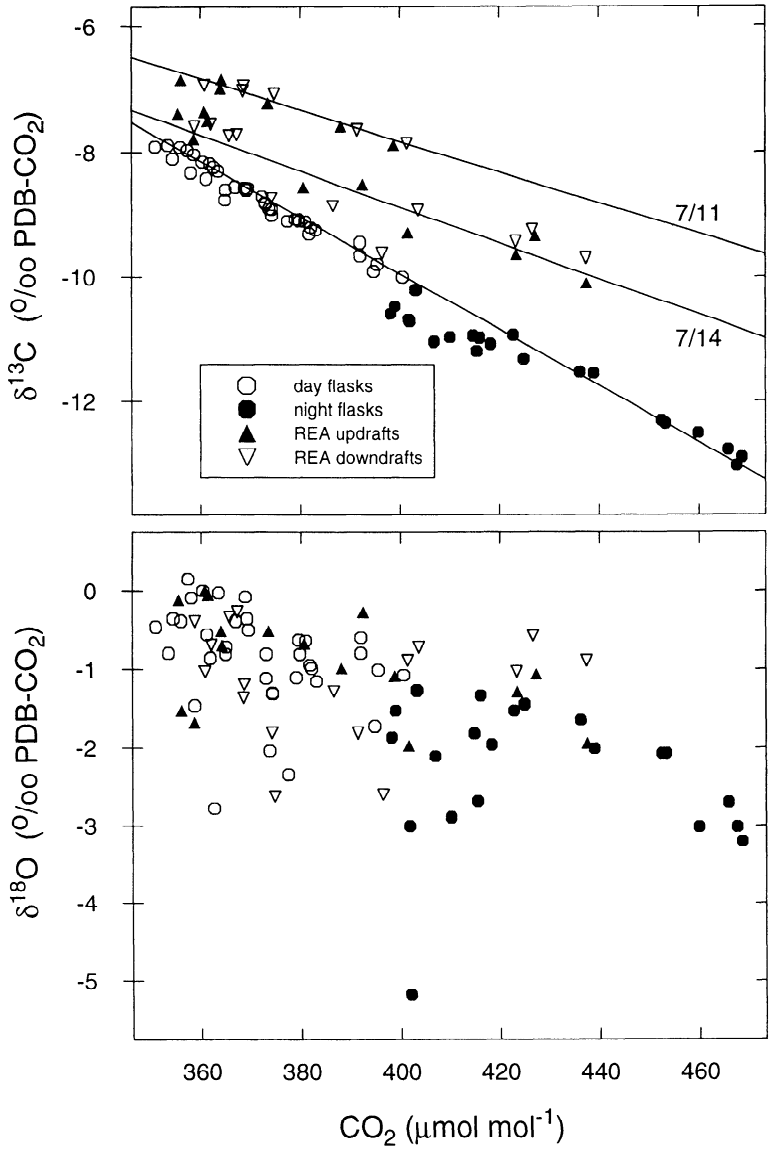

Figure 9. The $\delta^{13}C$ and $\delta^{18}O$ in CO_2 versus CO_2 mixing ratio. Flask data are whole-air samples and are divided into daylight (open circles, collected July 14, 15, and 17) and nocturnal (filled circles, collected July 13 and 14) periods. REA updraft and downdraft (up and down triangles) samples are shown for July 11 and 14 only. Distinct regression lines are apparent on each day for REA $\delta^{13}C$ data but not REA $\delta^{18}O$ data. Regression lines are drawn for daytime flasks and each REA day separately. Equations for these and other regressions are shown in Table 1.

ences in isotope ratio between updrafts and downdrafts could be improved by collecting whole-air samples rather than cryogenically extracting CO_2 at the time of updraft/downdraft segregation. An REA system designed to collect whole-air samples in flasks could take advantage of the analytical expertise of existing laboratories, where mass spectrometer precision for $\delta^{13}C$ and $\delta^{18}O$ in whole-air flask samples is an order of magnitude better than the collection precision of the present REA system [*Trolier et al.*, 1996; *Ehleringer and Cook*, 1998]. Collection of whole-air samples would also allow mixing ratio and isotope ratio determinations for the REA to be performed on the same samples. Given the complexities of the $\delta^{18}O$-versus-C relationship (Figure 9) and the large discrepancy between the EC/flask and REA fluxes for $C^{18}OO$ (Figure 11), it is likely that REA will be the only reliable method for measuring $C^{18}OO$ fluxes. Thus we feel that continued development of the REA technique is warranted.

The representativeness of flux measurements at a single location is difficult to assess, and run-to-run variability in eddy fluxes leads to larger error in individual measurement periods than in ensemble averages of those periods [*Wesely and Hart*, 1985; *Moncrieff et al.*, 1996]. We averaged the $^{13}CO_2$ flux data over the 5-day period to better bound our errors and show isotopic fluxes over an "average" July day at Walker

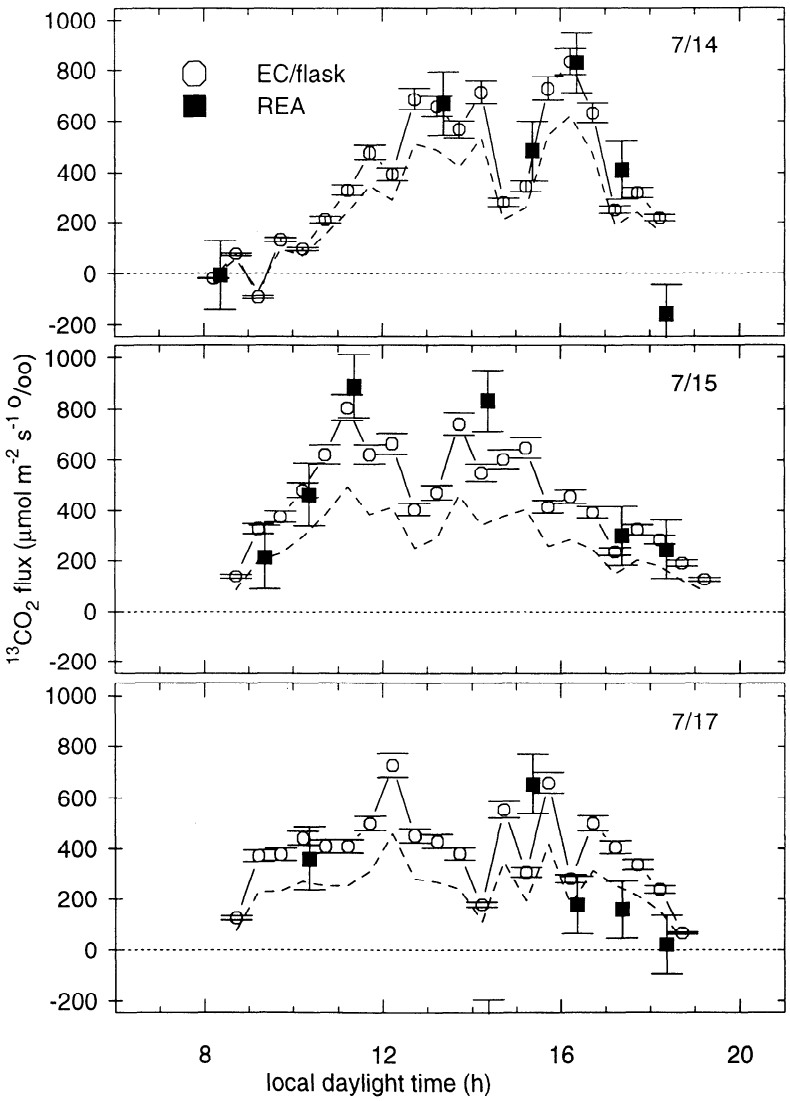

Figure 10. Eddy covariance/flask and REA fluxes of $^{13}CO_2$ (μmol m^{-2} s^{-1} ‰) for three REA sampling dates. EC/flask fluxes were calculated using equation (2) by combining δ^{13}C-versus-C regressions with fast w and CO_2 time series collected at 40 m. Shown are fluxes calculated with the overall daytime flask regression (circles) and each day's respective REA updraft/downdraft regression (dashed line). Regression equations are listed in Table 1. Error bars on the EC/flask measurements represent the 95% confidence intervals on the slope of the regression between δ^{13}C and CO_2 (these ignore errors in the eddy flux measurement, which can be estimated by averaging over repeated measurements as in Figure 12). Also shown are measured REA fluxes (equation (8)); error bars are calculated from measurement uncertainty in isotope ratio and mixing ratio of updrafts and downdrafts.

Branch (Figure 12). Note that overall conditions were fairly cloudy as net radiation rarely exceeded 600 W m^{-2}. NEE values, however, are typical for this forest in midsummer even under sunny conditions [*Baldocchi*, 1997], a pattern which likely reflects a change in leaf energy balance. Lower radiation load on the canopy under overcast skies decreases leaf temperatures and thus leaf respiration [*Baldocchi and Harley*, 1995], but total canopy carbon gain is enhanced because of the high availability of diffuse radiation [*Hollinger et al.*, 1994]. The diurnal pattern of ^{13}NEE tracks that of NEE very closely as expected, implying that the light response curve for ^{13}NEE is similar in shape to that for total CO_2 for this forest.

The sign of the isotopic fluxes in Figures 10-12 requires a cautionary note. Following our sign convention, a net gain of carbon by the forest is negative (NEE in Figure 12). Figure 12 implies that the direction of net $^{13}CO_2$ exchange is upward, which is incorrect. Our units for isotopic flux combine standard flux units (μmol m^{-2} s^{-1}) with standard isotopic units (‰) and are consistent with other studies [*Lloyd et al.*,

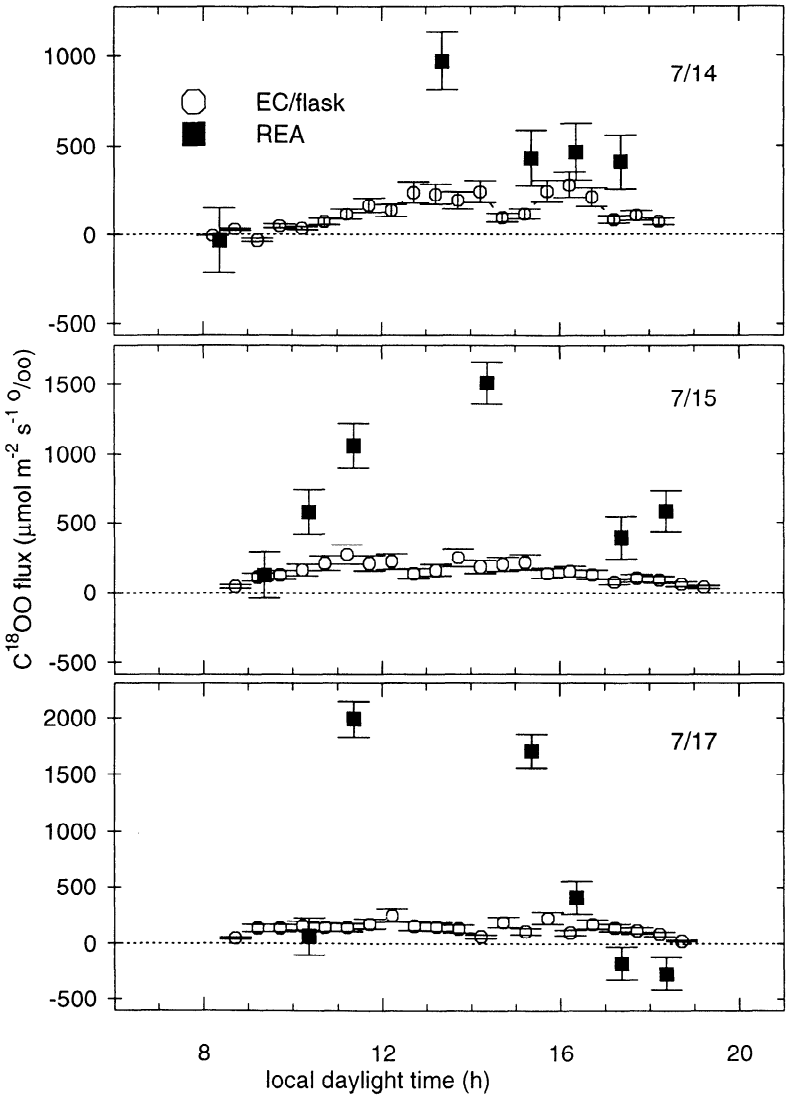

Figure 11. Eddy covariance/flask and REA fluxes of $C^{18}OO$ (μmol m^{-2} s^{-1} ‰) for three REA sampling dates. Eddy covariance fluxes were calculated using equation (2) modified for $\delta^{18}O$. Regression equations are listed in Table 1. Also shown are measured REA fluxes (equation (8) modified for $\delta^{18}O$). Error bars are as described in the caption of Figure 10.

1996; *Flanagan et al.*, 1997]. However, values for $\delta^{13}C$ and $\delta^{18}O$ in atmospheric CO_2 are negative due to the arbitrary choice of the international isotopic measurement standard (PDB carbonate). The above-canopy gradient in CO_2 and isotopic composition at midday (Figure 2) forces the gradient (and the flux direction) in $^{13}CO_2$ and $C^{18}OO$ mixing ratio to match that of total CO_2.

3.4. Heterogeneity in $\delta^{18}O$

The use of the EC/flask method to calculate isotopic fluxes for $C^{18}OO$ is not recommended because of the poor correlation between $\delta^{18}O$ and CO_2 (Figure 9, Table 1). Several other studies have noted considerable scatter in this relationship [e.g., *Nakazawa et al.*, 1997a,b; *Sternberg et al.*, 1998; *Harwood et al.*, 1999], while tighter correlations are apparent at some sites [*Flanagan et al.*, 1997; *Buchmann and Ehleringer*, 1998; *Ehleringer and Cook*, 1998]. These variations are likely due to spatial heterogeneity in the water pools that affect isotopic composition of CO_2, either through equilibration with unknown water sources such as dew or through species or community differences in leaf enrichment or soil water status. There was no precipitation at the Walker Branch field site during this study. However, there were strong isolated thunderstorms (typical of the summer precipitation pattern) within a few kilometers of the tower, which likely affected our tower measurements. The dependence of above-canopy $\delta^{18}O$ on wind direction (Figure 2), as well as the anomalous $\delta^{18}O$ patterns associated with the morning boundary layer transition suggest that oxygen isotope effects are not spatially uniform at the micrometeorological scale. There are distinct

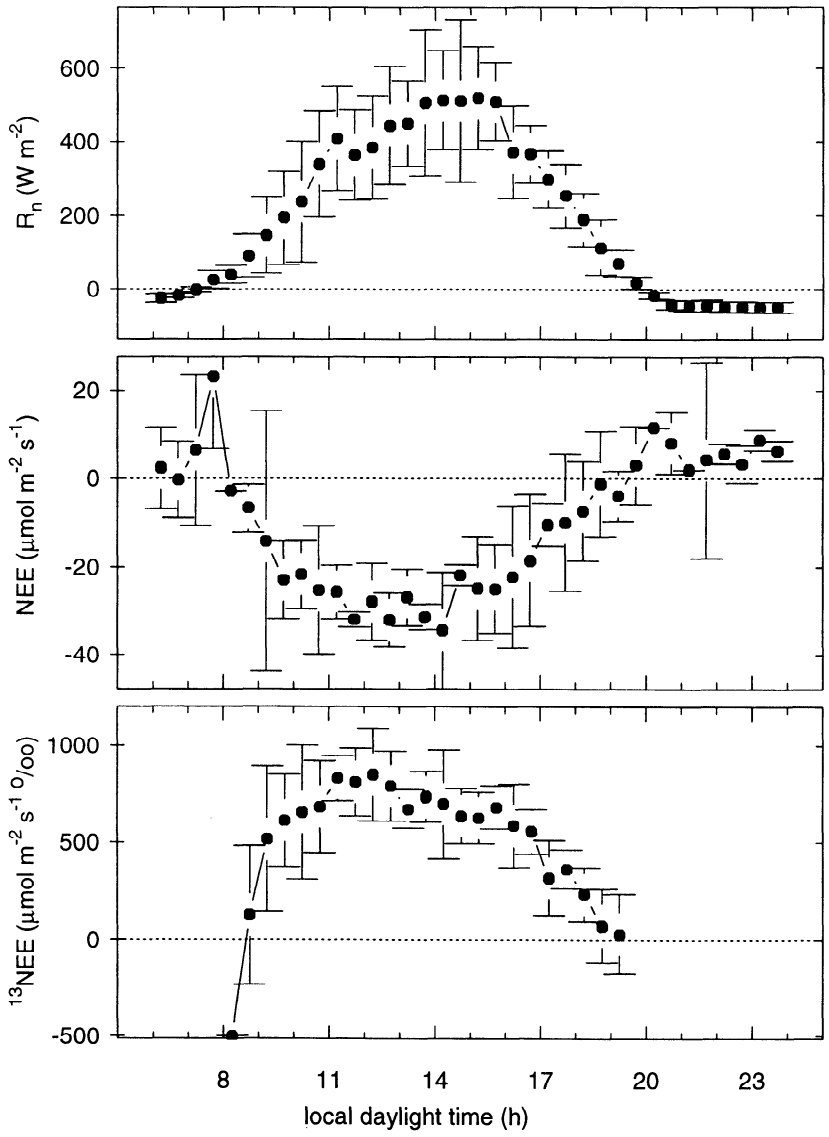

Figure 12. Half-hourly ensemble averages (error bars = $\pm 1\sigma$) over the five REA sampling dates for net radiation, total NEE (at 37 m), and $^{13}CO_2$ NEE (via EC/flask approach using daytime flask regression at 40 m, from Figure 10). Note the sign of the isotopic flux is misleading as discussed in the text.

patterns in $\delta^{18}O$ that are not apparent in CO_2 or $\delta^{13}C$ (Figures 2 and 8), suggesting that the forest within the tower footprint is more homogeneous with respect to discrimination against ^{13}C than for isotopic effects on ^{18}O. This is possibly true at other sites; anomalous diurnal patterns in $\delta^{18}O$ in or near the upper canopy have been reported by several groups [*Flanagan et al.*, 1997, Figures 4 and 5; *Nakazawa et al.*, 1997a, Figure 2; *Harwood et al.*, 1999, Figure 5]. However, the majority of diurnal patterns in $\delta^{18}O$ that have been reported do not show this anomalous behavior [*Flanagan and Varney*, 1995; *Flanagan et al.*, 1997].

Assuming that respired CO_2 is derived from recently fixed photosynthate, one unit of net carbon assimilation by the forest will have exactly the opposite effect on $\delta^{13}C$ in forest air as one unit of respiration. This implies that a unit change in $\delta^{13}C$ could be interpreted alternatively as an increase in A or a decrease in R (or vice versa). Due to the large difference in soil water and leaf water isotope ratio during the day, it is the oxygen isotopic signal in CO_2 that carries the most independent information about A and R. Since our ultimate goal is to use variations in isotopic composition to understand these biological processes, further effort to understand the biological and physical factors controlling variation in $\delta^{18}O$ and in fluxes of $C^{18}OO$ is warranted, despite the uncertainties associated with large-scale spatial heterogeneity.

3.5. Broader Implications

At present our understanding of the global carbon cycle is based in large part on interpreting seasonal changes in atmospheric $\delta^{13}C$, $\delta^{18}O$, and CO_2 using inversion modeling. A thorough understanding of the patterns of isotopic exchange

in terrestrial ecosystems is necessary if we are to interpret these variations quantitatively as an indicator of global sources and sinks of CO_2. The global sampling network is necessarily located at remote (mostly coastal) sites and hence regional interpretations of global patterns are controversial and relatively poorly constrained [*Fan et al.*, 1998]. Recent expansion of terrestrial CO_2 flux monitoring sites provides an additional constraint on the models, but isotopic information (and especially isotopic flux information) at virtually all of these sites is lacking. Besides the fluxes themselves, a critical element in inversion modeling studies is the value of photosynthetic isotope discrimination (Δ) at large scales. Attempts have been made to model this parameter [*Lloyd and Farquhar*, 1994; *Ciais et al.*, 1995; *Fung et al.*, 1997], but we have little experimental data to validate these estimates at canopy-to- larger scales [*Bakwin et al.*, 1998b].

Diurnal or seasonal changes in the ratio ^{13}NEE/NEE or ^{18}NEE/NEE should reflect changes in (1) whole-canopy photosynthetic discrimination and/or (2) the relative proportions of photosynthesis and respiration, and thus these ratios may serve as an indicator of photosynthetic discrimination at the ecosystem scale. Long-term studies are needed in a variety of ecosystems to examine how environmental variables affect isotopic exchange through influences on canopy conductance, soil moisture, decomposition rates, etc. Although the REA measurements described here are fairly labor-intensive and thus likely to be of limited use in a long-term study, the EC/flask technique is simple and can be extensively applied. Existing flux measurement programs could add minimal regular flask sampling to their suite of measurements and begin measuring $^{13}CO_2$ fluxes (and $C^{18}OO$ at some sites) for little additional cost. Such efforts should focus on (1) establishing the δ- versus-C and Keeling relations at relevant timescales (at least monthly), (2) determining whether biota at various canopy heights influence these relations differently (e.g., soil respiration versus overstory photosynthesis), (3) defining the physiological factors that influence these relations (e.g., stomatal conductance, differences in CO_2 assimilation rate, leaf water enrichment, etc.), and (4) using measurements of $\delta^{13}C$ in leaf and soil organics and $\delta^{18}O$ of leaf, soil, and stem water to assess spatial heterogeneity in isotope effects within the tower footprint. The nonuniformity of $\delta^{18}O$ in atmospheric CO_2 at the canopy scale may be a useful indicator of flux footprint if sufficiently characterized.

4. Conclusions

We used two new and independent techniques to provide the first direct measurements of net $^{13}CO_2$ and $C^{18}OO$ exchange over forests. We used these measurements to examine the dynamics of the isotopic composition of forest CO_2. From this study we draw several conclusions.

1. There are significant diurnal changes in carbon and oxygen isotopic composition of forest CO_2 that reflect the separate influences of net photosynthetic assimilation and ecosystem respiration. These are useful signals that are likely to provide new information about these processes provided they can be appropriately exploited.

2. Boundary layer growth and associated mixing have a strong controlling influence on the isotopic composition of CO_2 in a forest. Studies which seek to use stable isotopes to discern biological processes in terrestrial ecosystems must address these effects.

3. There are strong linear correlations between $\delta^{13}C$ and CO_2 that can be easily combined with standard eddy covariance data to compute net ecosytem exchange of $^{13}CO_2$. This approach is less robust for $C^{18}OO$ due to natural variability in the water pools that exchange isotopically with CO_2.

4. The HREA technique provided measurable differences in updraft and downdraft isotopic composition, despite the fact that the collection system precision was relatively poor. This precision can likely be improved if an REA system can be devised that collects updrafts and downdrafts as whole-air samples without isotopic fractionation.

Acknowledgments. We thank Pieter Tans, Jim White, and Dan Yakir for many useful ideas and discussions. Elise Pendall, Don Lenschow, Larry Flanagan, Bruce Vaughn, Tony Delany, Steve Oncley, and Andrew Turnipseed all helped with various intellectual aspects of this research. Tom Conway (NOAA/CMDL) and Candice Urban-Evans and Kim Elkins (University of Colorado/INSTAAR) kindly analyzed the flasks and performed the isotope analyses. Laura Scott, Marcy Litvak, Jeff Andrews, Andrew Turnipseed, Paul Hanson, and Mark Hall provided valuable assistance in the field. D.R.B. was supported during this time by U. S. Environmental Protection Agency Graduate Research Fellowship U-914722-01-1, and NSF Research Training Grant BIR-9413218. This research was equally funded by TECO NSF grant IBN9814507 and the National Institute for Global Environmental Change through the U.S. Department of Energy (Cooperative Agreement DE-FC03-90ER61010). Any opinions, findings, and conclusions or recommendations expressed in this publication are those of the authors and do not necessarily reflect the views of NSF or DOE.

References

Bakwin, P. S., P. P. Tans, D. F. Hurst, and C. Zhao, Measurements of carbon dioxide on very tall towers: Results of the NOAA/CMDL program, *Tellus Ser. B, 50*, 401-415, 1998a.

Bakwin, P. S., P. P. Tans, J. W. C. White, and R. J. Andres, Determination of the isotopic ($^{13}C/^{12}C$) discrimination by terrestrial biology from a global network of observations, *Global Biogeochem. Cycles, 12*, 555-562, 1998b.

Baldocchi, D., Measuring and modelling carbon dioxide and water vapour exchange over a temperate broad-leaved forest during the 1995 summer drought, *Plant, Cell, Environ., 20*, 1108-1122, 1997.

Baldocchi, D. D., and P. C. Harley, Scaling carbon dioxide and water vapour exchange from leaf to canopy in a deciduous forest, Part II, Model testing and application, *Plant, Cell, Environ., 18*, 1157-1173, 1995.

Baldocchi, D.D., B. B. Hicks, and T. P. Meyers, Measuring biosphere-atmosphere exchanges of biologically related gases with micrometeorological methods, *Ecology, 69*, 1331-1340, 1988.

Baldocchi, D. D., J. D. Fuentes, D. R. Bowling, A. A. Turnipseed, and R. K. Monson, Scaling isoprene fluxes from leaves to canopies: Test cases over a boreal aspen and a mixed species temperate forest, *J. Appl. Meteorol., 38*, 885-898, 1999.

Barr, A. G., and A. K. Betts, Radiosonde boundary layer budgets above a boreal forest, *J. Geophys. Res., 102*, 29,205-29,212, 1997.

Bowling, D. R., A. A. Turnipseed, A. C. Delany, D. D. Baldocchi, J. P. Greenberg, and R. K. Monson, The use of relaxed eddy accumulation to measure biosphere-atmosphere exchange of isoprene and other biological trace gases, *Oecologia, 116*, 306- 315, 1998.

Bowling, D. R., A. C. Delany, A. A. Turnipseed, D. D. Baldocchi, and R. K. Monson, Modification of the relaxed eddy accumulation technique to maximize measured scalar mixing ratios differences in updrafts and downdrafts, *J. Geophys. Res., 104*, 9121-9133, 1999.

Buchmann, N., and J. R. Ehleringer, CO_2 concentration profiles, and carbon and oxygen isotopes in C_3 and C_4 crop canopies, *Agric. For. Meteorol.*, *89*, 45-58, 1998.

Buchmann, N., J.-M. Guehl, T. S. Barigah, and J. R. Ehleringer, Interseasonal comparison of CO_2 concentrations, isotopic composition, and carbon dynamics in an Amazonian rainforest (French Guiana), *Oecologia*, *110*, 120-131, 1997.

Buchmann, N., T. M. Hinckley, and J. R. Ehleringer, Carbon isotope dynamics in *Abies amabilis* stands in the Cascades, *Can. J. For. Res.*, *28*, 808-819, 1998.

Businger, J. A., and S. P. Oncley, Flux measurement with conditional sampling, *J. Atmos. Oceanic Technol.*, *7*, 349-352, 1990.

Cellier, P., and Y. Brunet, Flux-gradient relationships above tall plant canopies, *Agric. For. Meteorol.*, *58*, 93-117, 1992.

Ciais, P., P. P. Tans, J. W. C. White, M. Trolier, R. J. Francey, J. A. Berry, D. R. Randall, P. J. Sellers, J. G. Collatz, and D. S. Schimel, Partitioning of ocean and land uptake of CO_2 as inferred by $\delta^{13}C$ measurements from the NOAA Climate Monitoring and Diagnostics Laboratory Global Air Sampling Network, *J. Geophys. Res.*, *100*, 5051-5070, 1995.

Conway, T. J., P. P. Tans, L. S. Waterman, K. W. Thoning, D. R. Kitzis, K. A. Masarie, and N. Zhang, Evidence for interannual variability of the carbon cycle from the National Oceanic and Atmospheric Administration/Climate Monitoring and Diagnostics Laboratory Global Air Sampling Network, *J. Geophys. Res.*, *99*, 22,831- 22,855, 1994.

Culf, A. D., G. Fisch, Y. Malhi, and C. A. Nobre, The influence of the atmospheric boundary layer on carbon dioxide concentrations over a tropical forest, *Agric. For. Meteorol.*, *85*, 149-158, 1997.

Davis, K. J., D. H. Lenschow, S. P. Oncley, C. Kiemle, G. Ehret, A. Giez, and J. Mann, Role of entrainment in surface-atmosphere interactions over the boreal forest, *J. Geophys. Res.*, *102*, 29,219-29,230, 1997.

Delany, A. C., D. R. Fitzjarrald, D. H. Lenschow, R. Pearson Jr., G. J. Wendel, and B. Woodruff, Direct measurements of nitrogen oxides and ozone fluxes over grassland, *J. Atmos. Chem.*, *4*, 429-444, 1986.

Dlugokencky, E. J., L. P. Steele, P. M. Lang, and K. A. Masarie, The growth rate and distribution of atmospheric methane, *J. Geophys. Res.*, *99*, 17,021-17,043, 1994.

Duranceau, M., J. Ghashghaie, F. Badeck, E. Deleens, and G. Cornic, $\delta^{13}C$ of CO_2 respired in the dark in relation to $\delta^{13}C$ of leaf carbohydrates in *Phaseolus vulgaris* L. under progressive drought, *Plant, Cell, Environ.*, *22*, 515-523, 1999.

Ehleringer, J. R., and C. S. Cook, Carbon and oxygen isotope ratios of ecosystem respiration along an Oregon conifer transect: Preliminary observations based on small- flask sampling, *Tree Physiol.*, *18*, 513-519, 1998.

Fan, S., M. Gloor, J. Mahlman, S. Pacala, J. Sarmiento, T. Takahashi, and P. Tans, A large terrestrial carbon sink in North America implied by atmospheric and oceanic carbon dioxide data and models, *Science*, *282*, 442-446, 1998.

Flanagan, L. B., J. P. Comstock, and J. R. Ehleringer, Comparison of modeled and observed environmental influences on the stable oxygen and hydrogen isotope composition of leaf water in *Phaseolus vulgaris* L, *Plant Physiol.*, *96*, 588-596, 1991.

Flanagan, L. B., and G. T. Varney, Influence of vegetation and soil CO_2 exchange on the concentration and stable oxygen isotope ratio of atmospheric CO_2 within a *Pinus resinosa* canopy, *Oecologia*, *101*, 37-44, 1995.

Flanagan, L. B., J. R. Brooks, G. T. Varney, S. C. Berry, and J. R. Ehleringer, Carbon isotope discrimination during photosynthesis and the isotope ratio of respired CO_2 in boreal forest ecosystems, *Global Biogeochem. Cycles*, *10*, 629-640, 1996.

Flanagan, L. B., J. R. Brooks, G. T. Varney, and J. R. Ehleringer, Discrimination against $C^{18}O^{16}O$ during photosynthesis and the oxygen isotope ratio of respired CO_2 in boreal forest ecosystems, *Global Biogeochem. Cycles*, *11*, 83-98, 1997.

Friedli, H., U. Siegenthaler, D. Rauber, and H. Oeschger, Measurements of concentration, $^{13}C/^{12}C$ and $^{18}O/^{16}O$ ratios of tropospheric carbon dioxide over Switzerland, *Tellus Ser. B*, *39*, 80-88, 1987.

Fung, I., et al., Carbon 13 exchanges between the atmosphere and biosphere, *Global Biogeochem. Cycles*, *11*, 507-533, 1997.

Giez, A., G. Ehret, R. L. Schwiesow, K. J. Davis, and D. H. Lenschow, Water vapor flux measurements from ground-based vertically-pointed water vapor differential absorption and Doppler lidars, *J. Atmos. Oceanic Technol.*, *16*, 237-250, 1999.

Goulden, M. L., J. W. Munger, S.-M. Fan, B. C. Daube, and S. C. Wofsy, Measurements of carbon sequestration by long-term eddy covariance: methods and a critical evaluation of accuracy, *Global Change Biol.*, *2*, 169-182, 1996.

Guenther, A. B., et al., Isoprene fluxes measured by enclosure, relaxed eddy accumulation, surface layer gradient, mixed layer gradient, and mixed layer mass balance techniques, *J. Geophys. Res.*, *101*, 18,555-18,567, 1996.

Hanson, P. J., D. E. Todd, M. A. Huston, J. D. Joslin, J. L. Croker, and R. M. Auge, Description and field performance of the Walker Branch Throughfall Displacement Experiment: 1993-1996, *ORNL/TM-13586*, Oak Ridge Nat. Lab., Oak Ridge, Tenn., 1998.

Harwood, K. G., J. S. Gillon, A. Roberts, and H. Griffiths, Determinants of isotopic coupling of CO_2 and water vapour within a (*Quercus petraea*) forest canopy, *Oecologia*, *119*, 109-119, 1999.

Hesterberg, R., and U. Siegenthaler, Production and stable isotopic composition of CO_2 in a soil near Bern, Switzerland, *Tellus Ser. B*, *43*, 197-205, 1991.

Hofmann, D. J., J. T. Peterson, and R. M. Rosson, Climate monitoring and diagnostics laboratory summary, *Rep. 24*, Nat. Oceanic and Atmos. Admin., Silver Spring, Md., 1998.

Hollinger, D. Y., F. M. Kelliher, J. N. Byers, J. E. Hunt, T. M. McSeveny, and P. L. Weir, Carbon dioxide exchange between an undisturbed old-growth temperate forest and the atmosphere, *Ecology*, *75*, 134-150, 1994.

Johnson, D. W., and R. I. van Hook (Eds.), *Analysis of Biogeochemical Cycling Processes in Walker Branch Watershed*, 401 pp., Springer-Verlag, New York, 1989.

Kaimal, J. C., and J. J. Finnigan, *Atmospheric Boundary Layer Flows, Their Structure and Measurement*, New York, Oxford Univ. Press, 289 pp., 1994.

Katul, G. G., P. L. Finkelstein, J. F. Clarke, and T. G. Ellestad, An investigation of the conditional sampling method used to estimate fluxes of active, reactive, and passive scalars, *J. Appl. Meteorol.*, *35*, 1835-1845, 1996.

Keeling, C. D., The concentration and isotopic abundances of atmospheric carbon dioxide in rural areas, *Geochim. Cosmochim. Acta.*, *13*, 322-334, 1958.

Lenschow, D. H., B. B. Stankov, and L. Mahrt, The rapid morning boundary-layer transition, *J. Atmos. Sci.*, *36*, 2108-2124, 1979.

Lin, G., and J. R. Ehleringer, Carbon isotopic fractionation does not occur during dark respiration in C_3 and C_4 plants, *Plant Physiol.*, *114*, 391-394, 1997.

Lloyd, J., and G. D. Farquhar, ^{13}C discrimination during CO_2 assimilation by the terrestrial biosphere, *Oecologia*, *99*, 201-215, 1994.

Lloyd, J., et al., Vegetation effects on the isotopic composition of atmospheric CO_2 at local and regional scales: theoretical aspects and a comparison between rain forest in Amazonia and a boreal forest in Siberia, *Aust. J. Plant Physiol.*, *23*, 371-399, 1996.

Martin, C. L., D. Fitzjarrald, M. Garstang, A. P. Oliveira, S. Greco, and E. Browell, Structure and growth of the mixing layer over the Amazonian rain forest, *J. Geophys. Res.*, *93*, 1361-1375, 1988.

McMillen, R. T., An eddy correlation technique with extended applicability to non-simple terrain, *Boundary-Layer Meteorol.*, *43*, 231-245, 1988.

Miller, J. B., D. Yakir, J. W. C. White, and P. Tans, Measurement of $^{18}O/^{16}O$ in the soil- atmosphere CO_2 flux, *Global Biogeochem. Cycles*, *13*, 761-774, 1999.

Moncrieff J. B., Y. Malhi, and R. Leuning, The propogation of errors in long-term measurements of land-atmosphere fluxes of carbon and water, *Global Change Biol.*, *2*, 231-240, 1996.

Nakazawa, T., S. Murayama, M. Toi, M. Ishizawa, K. Otonashi, S. Aoki, and S. Yamamoto, Temporal variations of the CO_2 con-

centration and its carbon and oxygen isotopic ratios in a temperate forest in the central part of the main island of Japan, *Tellus Ser. B, 49*, 364-381, 1997a.

Nakazawa, T., S. Sugawara, G. Inoue, T. Machida, S. Makshyutov, and H. Mukai, Aircraft measurements of the concentrations of CO_2, CH_4, N_2O, and CO and the carbon and oxygen isotope ratios of CO_2 in the troposphere over Russia, *J. Geophys. Res., 102*, 3843-3859, 1997b.

Nie, D., T. E. Kleindienst, R. R. Arnts, and J. E. Sickles II, The design and testing of a relaxed eddy accumulation system, *J. Geophys. Res., 100*, 11,415-11,423, 1995.

Novelli, P. C., K. A. Masarie, and P. M. Lang, Distributions and recent changes of carbon monoxide in the lower troposphere, *J. Geophys. Res., 103*, 19,015-19,033, 1998.

Novelli, P. C., L. P. Steele, and P. P. Tans, Mixing ratios of carbon monoxide in the troposphere, *J. Geophys. Res., 97*, 20,731-20,750, 1992.

Pattey, E., R. L. Desjardins, F. Boudreau, and P. Rochette, Impact of density fluctuations on flux measurements of trace gases: implications for the relaxed eddy accumulation technique, *Boundary-Layer Meteorol., 59*, 195-203, 1992.

Sternberg, L. S. L., M. Z. Moreira, L. A. Martinelli, R. L. Victoria, E. M. Barbosa, L. C. M. Bonates, and D. C. Nepstad, Carbon dioxide recycling in two Amazonian tropical forests, *Agric. For. Meteorol., 88*, 259-268, 1997.

Sternberg, L. S. L., M. Z. Moreira, L. A. Martinelli, R. L. Victoria, E. M. Barbosa, L. C. M. Bonates, and D. C. Nepstad, The relationship between $^{18}O/^{16}O$ and $^{13}C/^{12}C$ ratios of ambient CO_2 in two Amazonian tropical forests, *Tellus Ser. B, 50*, 366-376, 1998.

Stull, R. B., *An Introduction to Boundary Layer Meteorology*, 666 pp., Kluwer Acad., Norwell, Mass., 1988.

Tans, P. P., Oxygen isotopic equilibrium between carbon dioxide and water in soils, *Tellus Ser. B, 50*, 163-178, 1998.

Trolier, M., J. W. C. White, P. P. Tans, K. A. Masarie, and P. A. Gemery, Monitoring the isotopic composition of atmospheric CO_2: Measurements from the NOAA Global Air Sampling Network, *J. Geophys. Res., 101*, 25,897-25,916, 1996.

Valentini, R., S. Greco, G. Seufert, N. Bertin, P. Ciccioli, A. Cecinato, E. Brancaleoni, and M. Frattoni, Fluxes of biogenic VOC from Mediterranean vegetation by trap enrichment relaxed eddy accumulation, *Atmos. Environ., 31*, 229-238, 1997.

Wang, X.-F., and D. Yakir, Temporal and spatial variations in the oxygen-18 content of leaf water in different plant species, *Plant, Cell, Environ., 18*, 1377-1385, 1995.

Webb, E. K., G. I. Pearman, and R. Leuning, Correction of flux measurements for density effects due to heat and water vapour transfer, *Q. J. R. Meteorol. Soc., 106*, 85-100, 1980.

Wesely, M. L., and R. L. Hart, Variability of short term eddy-correlation estimates of mass exchange, in *The Forest-Atmosphere Interaction*, edited by B. A. Hutchinson and B. B. Hicks, pp. 591-612., D. Reidel, Norwell, Mass., 1985.

Williams, T. G., L. B. Flanagan, and J. R. Coleman, Photosynthetic gas exchange and discrimination against $^{13}CO_2$ and $C^{18}O^{16}O$ in tobacco plants modified by an antisense construct to have low chloroplastic carbonic anhydrase, *Plant. Physiol., 112*, 319-326, 1996.

Yakir, D., and X.-F. Wang, Fluxes of CO_2 and water between terrestrial vegetation and the atmosphere estimated from isotope measurements, *Nature, 380*, 515-517, 1996.

D. D. Baldocchi, Department of Environmental Science, Policy and Management, 354 Hilgard Hall, University of California, Berkeley, CA 94720. (baldocchi@nature.berkeley.edu)

D. R. Bowling, Department of Biology, University of Utah, 257 South 1400 East, Salt Lake City, UT 84112-0840. (bowling@biology.utah.edu)

R. K. Monson, Department of Environmental, Population, and Organismic Biology, University of Colorado, Campus Box 334, Boulder, CO 80309. (monsonr@colorado.edu)

(Received April 27, 1999; revised August 11, 1999; Accepted August 24, 1999.)